Scientific Reports

https://doi.org/10.1038/s41598-026-39172-5

Article in Press

Investigation of hydrogen influence on compression ignition engine fuelled with pyrolysis blends using experimental and RSM methods

Received: 4 May 2025

Accepted: 3 February 2026

Published online: 24 February 2026

Cite this article as: Kumar K.S., Surakasi R., Kareemullah M. *et al.* Investigation of hydrogen influence on compression ignition engine fuelled with pyrolysis blends using experimental and RSM methods. *Sci Rep* (2026). https://doi.org/10.1038/s41598-026-39172-5

K. Sunil Kumar, Raviteja Surakasi, Md Kareemullah, Sarfaraz Kamangar, Amir Ibrahim Ali Arabi & Addisu Frinjo Emma

Investigation of Hydrogen Influence on Compression Ignition Engine Fuelled with Pyrolysis Blends Using Experimental and RSM Methods

1* K. Sunil Kumar, [2] Raviteja Surakasi**,** Md Kareemullah[3, 4], Sarfaraz Kamangar[5], Amir Ibrahim Ali Arabi[5], Addisu Frinjo Emma[6*]

[1*]Department of Mechanical Engineering, Saveetha School of Engineering, Saveetha Institute of Medical and Technical Sciences, Chennai,602105, Tamil Nadu, India.

[2]Department of Mechanical Engineering, Lendi Institute of Engineering and Technology
Jonnada, Vizianagaram, Andhra Pradesh- 535005,raviteja.surakasi@lendi.org

[3]Department of Mechanical Engineering, Graphic Era (Deemed to be University), Dehradun-248002, Uttarakhand, India.
mdkareemullah25@gmail.com

[4]Centre of Research Impact and Outcome, Chitkara University, Rajpura 140417, Punjab, India.

[5]Mechanical Engineering Department, College of Engineering, King Khalid University, Abha 61421, Saudi Arabia. sarfaraz.kamangar@gmail.com, aarabi@kku.edu.sa

[6]College of Engineering and Technology, School of Mechanical and Automotive Engineering, Dilla University, Gedeo Zone, South Ethiopia Regional State, Po. Box 419, Dilla, Ethiopia.

*Correspondence: addisuf@du.edu.et, sunilkumarkresearcher@gmail.com

Abstract

This study experimentally investigates the performance, combustion, and emission characteristics of a single-cylinder diesel engine operated in dual-fuel mode using pyrolysis oil and gaseous hydrogen. Four fuel combinations were examined: neat diesel (100D), diesel–hydrogen (50D50H), diesel–pyrolysis oil (90D10P), and diesel–pyrolysis oil with hydrogen enrichment (90D10P + 50 LPH). The engine was operated at a constant speed of 1,500 rpm under varying load conditions (0–100%), and the results were analysed using response surface methodology (RSM). The 50D50H blend achieved the highest brake thermal efficiency, showing a 21.4% improvement over neat diesel, along with a minimum brake-specific fuel consumption of 0.22 kg/kWh. The maximum in-cylinder pressure (69 bar) and peak heat release rate (75 J/°CA) were observed for the 90D10P + 50 LPH blend. Emission analysis indicated that this blend produced the lowest carbon monoxide, carbon dioxide, hydrocarbon, and nitrogen oxide emissions among all tested fuels, while the lowest NO_x emission of 350 ppm was recorded for the 50D50H blend. Statistical validation using

analysis of variance (ANOVA) yielded regression coefficients (R^2) between 0.8 and 1, demonstrating strong agreement between experimental results and model predictions. The findings confirm that the combined application of pyrolysis oil and hydrogen in dual-fuel operation significantly enhances engine efficiency while effectively reducing exhaust emissions.

Keywords: Hydrogen gas; Pyrolysis oil; Dual engine; Response surface methodology; Green energy.

INTRODUCTION

The use of CI engines has gained significant attention due to their robust and efficient design. However, particulate emissions from these engines remain a pressing global concern [1]. Nitrogen oxides (NOx) and particulate matter are the primary pollutants emitted by internal combustion engines. Incorporating alternative fuels such as alcohols has shown potential in improving emission profiles of compression ignition engines while reducing fossil fuel dependency and mitigating resource depletion [2]. Recent advancements have explored hydrogen gas as a supplementary fuel to enhance the speed, power, and fuel economy of compression ignition engines while simultaneously reducing emissions [3]. Studies suggest that hydrogen-diesel blends improve engine performance metrics such as torque and power, with hydrogen supplementation notably enhancing combustion characteristics [4-6]. For instance, continuous hydrogen flow at 5 LPM in a diesel engine demonstrated improved brake thermal efficiency but, at critical engine speeds like 1760 rpm, adversely affected torque and power due to combustion dynamics [7].

The primary benefits of utilizing hydrogen energy in a diesel engine, whether via twin-fuel operation or hydro-enriched burning, includes the Enhanced Burning Effectiveness, Hydrogen has a rapid flame velocity and an extensive ignition spectrum, resulting in enhanced effectiveness and expedited burning. This leads to enhanced combustion effectiveness and lower timing delays relative to solely diesel performance. The introduction of gas enhances the brake thermal efficiency (BTE) due to stronger

combustion and less loss of warmth. Hydrogen facilitates the attainment of reduced air-fuelled mixes, enhancing the car's energy use effectiveness [8]. Decrement in greenhouse gas emissions, The gas hydrogen is devoid of carbon, hence it lacks CO_2, CO, or uncombusted compounds (HC). This considerably decreases emissions of carbon dioxide in comparison to fuel made from diesel. Reduced Emissions of Nicotine and Particulates (PM). Hydrogen facilitates the thorough degradation of the combustible composition. The lack of atoms in protons prevents dirt and particle generation, leading to cleaner airborne pollutants. The low ignition potential of protons improves combustion dependability, particularly in weak or quick start situations [9]. This results in enhanced powertrain functionality and improved start-up efficiency. Potential for lean burner operations Hydrogen facilitates highly efficient burning owing to its extensive explosiveness range. Lean operating decreases burning warmth, hence potentially reducing atmospheric nitrogen oxides when properly tuned. In dual engines, a portion of the exhaust is substituted by gas. Due to the substance's efficient combustion, overall diesel consumption diminishes, enhancing the environment. The elevated energy density of the gas, which is approximately 100 -120 MJ/kg, facilitates greater energy discharge throughout fire, hence enhancing total engine productivity when effectively regulated. Peroxide can be generated from sources of clean electricity, such as sunshine or wind breakdown, thereby diminishing reliance on oil and gas and promoting longevity [10].

The disadvantages of hydrogen in the field of internal combustion engines includes, hydrogen possesses a low volumetric energy density, despite its large energy content per kilograms. It necessitates tanks with elevated pressures or freezing storage, hence augmenting equipment cost, weight, and sophistication. Hydrogen is extremely combustible and readily disintegrates, resulting in considerable dangers of spillage and detonation. Elevated NOx Pollution at enriched combinations The burning of hydrogen generates elevated flames intensities. excessive consumption of hydrogen might result in elevated NOx production due to increasing burning heat [11]. Rigorous regulation of mixing intensity (lean functioning) is essential

to mitigate the production of NOx. Prepping for Ignition and Detonation The gas hydrogen possesses low ignition impulse and elevated flame rapidity, potentially resulting in prematurely combustion, malfunctioning, or engine rattle. This impacts engine longevity and necessitates precise throttle regulation and specialized injection systems. Decreased Energy Delivery (in Certain Instances) Due to protons being held as a substance, it eliminates a portion of the inlet air, so diminishing the quantity of oxygen suitable for burning. This may result in diminished performance if not adequately tuned or accelerated. Amendment Specifications Traditional diesel engines are not engineered for fuel cell utilization. Hydrogen injection regulation devices, protection valves, gauges, and automation mechanisms must be fitted as supplementary elements. The expenses associated with upgrading might be substantial and necessitate intricate calibrated. The extraction of gas via electroplating or restructuring can be costly and demanding on energy, particularly when utilizing renewable sources [12].

Hydrogen incorporation has also been studied with biodiesel blends. Research. revealed that diesel-hydrogen blends achieved higher torque and power, alongside a 9% improvement in brake torque and a 10% reduction in emissions compared to conventional diesel. Studies on B15 biodiesel combined with hydrogen showed a marked reduction in particulate emissions. Electrolysis-derived hydrogen, when blended with Moringa oleifera biodiesel, led to a 6% reduction in pollutants relative to other fuels. Further investigations into hydrogen application in common rail direct injection (CRDI) engines highlighted performance and emission improvements [13]. Experiments involving hydrogen gas injection into the intake manifold demonstrated reduced pollutants and enhanced efficiency. Research with biodiesel derived from vegetable oil and hydrogen supplementation in a direct injection engine confirmed similar positive trends. Dual-mode engine operations utilizing hydrogen and diesel, with or without dimethyl biodiesel, have shown up to a 5% improvement in performance and a 3% reduction in total emissions [14]. Studies also

indicate that hydrogen supplementation enhances brake thermal efficiency and reduces maintenance needs [15]. Theoretical analyses using Diesel-RK software revealed a 32% efficiency improvement with B10 blends at varying engine speeds. Innovative methodologies such as the Box-Behnken design have minimized experimental trials while optimizing hydrogen-diesel blends for lean operation and reduced emissions [16]. The "Hydrogen Boost" approach [17] demonstrated a significant reduction in hazardous particulates compared to pure gasoline. An experimental study [18] combining 20% palm biodiesel and 80% diesel with hydrogen in a dual-mode, oxygen-enriched combustion system used the Taguchi method and response surface methodology. The optimized conditions achieved through orthogonal arrays and variance analysis yielded substantial improvements in performance and emissions.

Biodiesel was initially included in fuels made from petroleum to mitigate pollutants and decrease reliance on crude oil. Numerous research have been undertaken to examine the impacts [19]. The utilization of biodiesel in compression ignition engines has been shown to diminish emissions and enhance engine performance. The oil is derived from diverse sources, including vegetable oils, animal fats, and used cooking oils [20]. It has been observed to increase NOx emissions. This results from the elevated oxygen concentration in biodiesel, which causes increased combustion temperatures and elevated NOx emissions. The objective of this investigation is to examine the diesel engine utilizing gaseous hydrogen and pyrolysis oil for combustion in dual mode, employing RSM and ANOVA approaches for a more comprehensive analysis of the results.

The novelty of this work comprises many researchers worked on dual engine followed by soyabeen blends and hydrogen, tamarind blends and hydrogen, palm blends and hydrogen and sunflower blends with hydrogen [21,22,23]. But the research is limited to plastic pyrolysis and hydrogen gas, hence in this research, the research gap and novelty of this work is pyrolysis oil with hydrogen to determine the engine characteristics concerned to performance, combustion and emissions. The burning

phasing, starting, and internal reactions involving protons has numerous benefits in terms of hydrogen significantly alters flame velocity, ignition characteristics, and combustion rate. The interaction of hydrogen furthermore, whether as augmentation or as a specialised atmospheric pilot, with pyrolysis fluid combustion delay, predetermined percentage, pre-ignition/knock, and heat transfer in various ignition modes is inadequately documented throughout operational maps. Enduring durability, substances, and accumulations. The porous and acidic materials in pyrolysis oil, along with the presence of hydrocarbons and potentially elevated burning levels, introduce uncertainties regarding the resilience of ring pistons, ignition actuators, and post-treatment systems concerned to limited prolonged performance trials. The meaning of dual mode in CI engine used in this analysis represents Diesel energy serves as the principal fuel, igniting combustion owing to its elevated cetane number. Pyrolysis oil, derived from leftover plastics, serves as an alternative or supplement fuel, being blended or integrated to partially substitute diesel. The amalgamation leverages diesel's burning consistency alongside the sustainable and cost-effective attributes of decomposing oil. Dual-mode fuels in a compression ignition engine (diesel + pyrolysis oil) denote a working phase wherein typical diesel and unconventional pyrolysis oil are utilized concurrently, through combined mixes or through distinct injection, to attain productive, healthier and more affordable burning capability.

Materials and Methods

Materials

The substance utilized for this investigation is hydrogen gas, which is contained within an insulated tank. The resulting pyrolysis oil is acquired from a local supplier in Hyderabad. The dealer is provided a low pricing amounting to 70 per litre for carrying out various trials and testing. The researchers incur a transport expense of five hundred rupees from the city of Hyderabad to Chennai. The extraction of pyrolysis oil from different plastics has been utilised in this analysis. The recovered pyrolysis oil from

various plastic sources undergoes transesterification using KOH and a 10% solution of methanol to eliminate trace amounts of sulphur contained in the pyrolysis oil. The chemical agents like chlorine are employed at a concentration of 3 to 5% to enhance the purification of pyrolysis oil, as its strong odour and high density adversely affect engine efficiency. The existing research indicates that elevated densities produce significant vibrations, adversely impacting engine performance. This leads to suboptimal outcomes and necessitates numerous experiments in uncertainty, possibly resulting in substantial random mistakes. To circumvent the numerous manipulations of pyrolysis oil, such as transesterification and chromatography, the sludge removal procedure is fundamentally executed before the investigation. The characteristics of the resulting hydrogen gas are delineated in Table 1. The pyrolysis standards are delineated in Table 2.

Table 1. Hydrogen gas properties

S NO	Properties	Units	Hydrogen gas
1	Low heat combustion	MJ/kg	121.22
2	Diffusivity coefficient	cm^2/s	0.66
3	Temperature Ignition	K	891
4	Ignition combustive	MJ	0.06
5	Flammability Limits by vol		5–79
6	Specific Heat	(kcal/kg °C)	3.55
7	Volumetric Composition	%	31.11
8	Air fuel mass ratio		0.041
9	Flame temperature	K	2330
10	Flame Speed	m/s	2.2
11	Stoichiometric Mixture	MJ	4.1
12	Quench parameter	mm	0.88
13	Liberative heat	MJ	3.41
14	High combustion property	MJ/kg	143.1
15	Densities	kg/m^3	0.084

Table 2. Properties of Pyrolysis oil and diesel

S No	Properties	Units	IS 1448	D6751	EN14214	100D	90D10P	100P
1	Iodine value	g	–	–	120	80	96	–
2	Flash point	°C	120	70	90	61	70.4	58
3	Acid value	mg	0.50	0.50	0.50	0.62	0.264	0.7
4	Cetane number	–	51	47	51	48	47.6	50
5	Kinematic viscosity @40 °C	cSt	2.5–6	2–6.5	3.5–5	2.91	3.074	4.38
6	Density	kg/m^3	860–900	800-890	0.86-.90	841	835	836
7	Calorific value	MJ/kg	45	45	46	44.94	43.7	38.75

Methods

Piezoelectric Cylinders Pressure Sensor (AVL GH14D) Quantifies contemporaneous inside-cylinder pressures throughout burning. This sensor Characteristics includes high-frequency responsiveness (up to 110 kHz) is crucial for detecting quick rising pressures resulting from hydrogen vapor's swift burning. Installed parallel with the gas chamber wall, typically via a slotted port on the engine's heads. The Charge Amplifier (Kistler Type 5011B) transforms the transducers electrically charged signals into a quantifiable signal. It purifies and regulates the unrefined signals. Maintains a steady zero standard across extended testing periods. The Crank angle encoder (Kubler 8.5820) precisely gauges the driveshaft position for synchronizing information regarding pressure with the rotational angle. The degree of accuracy of this actuator usually lies between 0.1 degrees and 1 degree of angle of cranks. It is affixed to the engine with a synchronization referencing indication generated by the highest centre of gravity identification. The Data Collection Equipment concurrently captures pressures and turn angle statistics. Recording frequency ≥ one hundred kHz to accurately record intricate tension patterns per turn of revolution. Conventional applications for software comprise interactions between transducers, amplifiers, and encoders. Low-Pass Digital filter eliminates powerful vibrations as well as noise from

the raw force output. The maximum acceptable frequency can vary from one to five kilohertz. The rationale for screening is that HHO burning generates rapid variations; screening guarantees a straight-line devoid misrepresenting actual spike.

EXPERIMENTAL SETUP AND EXPERIMENTAL PROCEEDURE

The experimental tests have been carried out with diesel operated single cylinder engine with four strokes on dual mode. This injection system is direct and cooled with water made by Kirloskar, India.

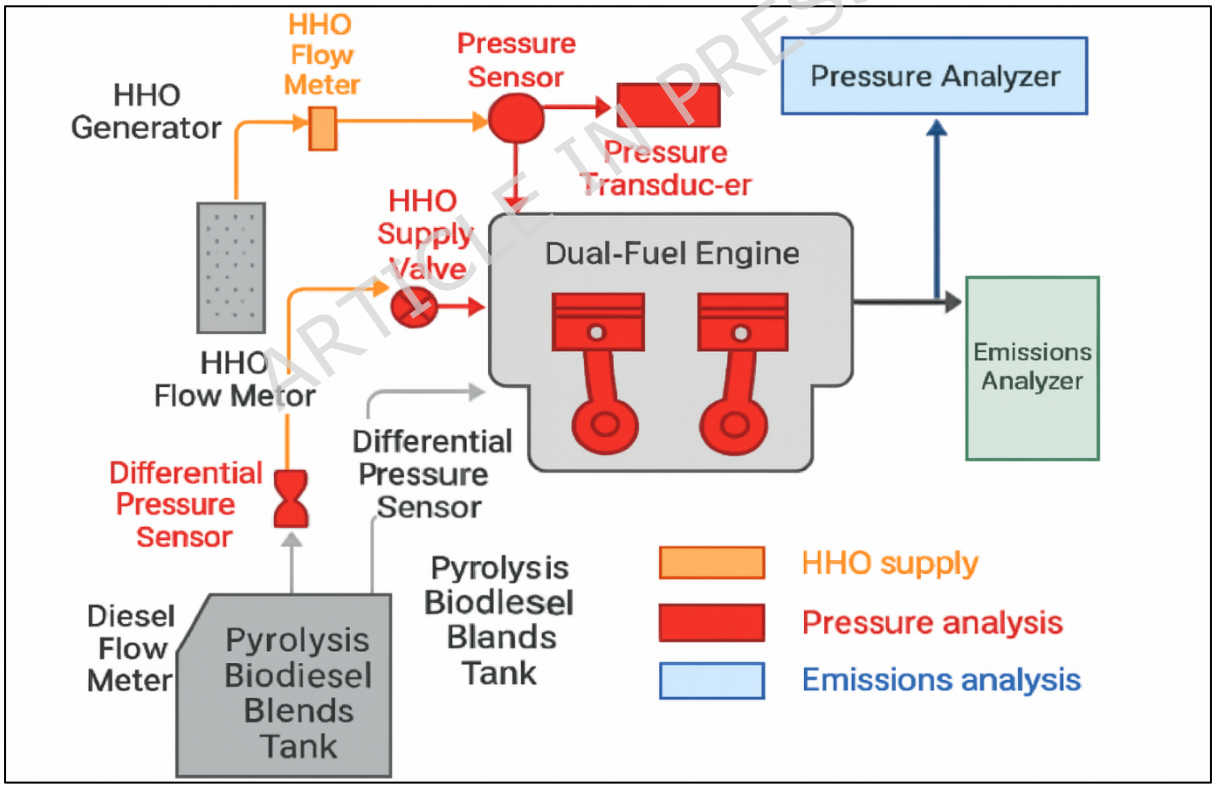

Figure 1. Line diagram of the Set-up

The Figure 1 illustrates a dual-fuel engine that is built specifically to function on regular diesel oil in conjunction with pyro blends consisting of

and supplementary hydrogen atoms oxyhydrogen gas. The above arrangement is characteristic of piston-injection system, wherein pyrolysis oil with different proportions serves as the principal fuel, while HHO is used to improve the combustion rate and diminish pollutants. During the examination, which encompassed various fuel discrepancies under varied output power levels, ranging from zero to the maximum output strength in twenty-five percent increments, the combustion engine operated constantly at 1500 rpm. The trials employed in a diesel engine. The engine features a stroke of 100 mm, a bore of 130 mm, with a compression ratio of 20:1, and is configured as an in-line, two-cylinder four-stroke system with fuel injection and water-cooled operation. An ordinary edge aperture on the lateral aspect of the ventilation box was employed to assess the airflow rate to mitigate fluctuations in the circulation of air, and a U-tube man was applied to gauge the weight differential across the opening. The type K thermostats were employed to assess the temperatures of the inhaled air and emissions gases. The prototype smoke coverage detector detects from zero to one hundred per cent with an accurate measurement of 0.1 percent and was utilized to assess the released haze. The engine exhaust gas analyser was employed for evaluating combustion contaminants within one of the following parameters: hydrocarbons (0 to 10000 ppm), O_2 (0 to twenty-five percent), CO (0 to twenty percent), CO_2 (0 to twenty percent), NOx (0 to five thousand ppm), λ (zero to 2), and AFR (0 to 98). Cylinder pressures were regulated throughout the tests, transitioning from zero to maximum at a steady speed rating of 1000 rpm. To get reliable measurements at a small variance, all engine efficiency and emission testing took place thrice. To maintain the engine under continuous demands, it was originally driven with loading approximately a half hour utilizing diesel fuel. prior to taking observations. The engine was subsequently subjected to the pyrolysis oil mixtures with different proportions 100D (100 % diesel), 50D50H (50% diesel and 50% hydrogen gas), 90D10P (90% diesel and 10% pyrolysis oil), and 90D10P+50 LPH (90% diesel, 10% pyrolysis oil, and 50 liters per hour of hydrogen gas) operating in dual mode. The experiment is conducted on 200 bar in 25º

BTDC and duration of injection is 2.5 ms. During the test, the designated frequency was sustained at 1500 revolutions per minute whilst the apparatus was adjusted from nothing to carry to full weight. The engine had originally heated up employing solely pure diesel energy void of any supplementary effort before the emissions temperatures stabilized. Table 3 represents engine setup.

Table 3. Engine Experiment Setup

Sno	Description	Units	Dimensions
1	Bore Diameter	mm	130
2	stroke	mm	100
3	Speed	rpm	2210
4	Torque	Nm	220
5	Speed	rpm	1500
6	Compression Ratio	-	20 :1

Initially, pure diesel has been used for warming up the engine. Throughout the study, the engine is subjected to incremental loads of 25 %, 50 %, 75 %, and 100 % with full load capacity of 220 Nm. At each load, once the engine reached a steady state, the temperature readings of the outlet water cooler and exhaust gas were recorded. The fuel flow is quantified using a calibrated hundred-millilitre division burette and a timer. The combustion airflow along the instrumentation of the gases analyser and smoking meter is utilized to measure the hydrogen gas discharge is assessed using a gas converter connected to a valve. The gas circulation meter measures the circulation trajectory of hydrogen. The fuel injector strength tester measures injection pressure, with variations achieved by deceiving the injector screw through tightening. Figure 2 displays a photographic reproduction belonging to the engine that powers the experimental instrument. Table 4 defines the steps involved in experimental methodology procedure.

Table 4. Steps involved in experimental methodology procedure

Steps	Actions	90D10WPO	D100	90D10WPO + H_2 (50 LPH	WPO100	Observations
1	Build labeled vessel	Prepare 90:10 v/v blend in labelled tank; mix	Fill D100 tank	Use same 90D10WPO blend tank; H_2 supply ready	Fill WPO tank; filter & preheat	Volume concerntrations
2	Sort out and warm	Filter (11–26 µm); preheat if viscosity high	Not required (normal diesel)	Same as 90D10WPO	Filter (10–25 µm); preheat to match injector limits	Temperature of preheats
3	Evaluation of fuel circulation meters	Calibrate for blend viscosity	Calibrate for diesel	Calibrate liquid meter; verify H_2 MFC/volumetric readout	Calibrate for WPO viscosity	Utilize Coriolis if accessible.
4	Engine preheating	Switch fuel lines, purge, stabilize	Warm on D100 20–30 min	Switch to 90D10WPO, then enable H_2 flow ramp	Purge & run at low load, monitor smoke	Allow coolant and intake temperatures to stabilize.
5	Establish operational parameters	Same	Set rpm & load	Same, then ramp H_2 to 50 LPH slowly	Same	Observe for inconsistency or knocking
6	Balance	Wait 10–15 min (blend equilibration)	Wait 5–10 min	After H_2 ramp, wait until stable several minutes	Wait 10–15 min, monitor injector behavior	Maintain consistent
7	Data collection	Same	Acquire 60–180 s steady data; ≥100 cycles	Acquire same + log H_2 flow continuously	Shorter runs recommended for WPO100 (inspect injectors often)	Preserve raw files with synchronized timestamps

8	Recurrent executions	Repeat ×3	Repeat ×3	Repeat ×3; confirm H_2 shutoff between repeats	Repeat ×2–3 (inspect injectors between runs)	Record anomalies
9	Terminate and eliminate	Purge lines or drain	Normal shutdown	Close H_2, purge manifold per procedure	Purge lines; clean filter	Document conclusive verifications

Figure. 2 Actual Experimental setup

Uncertainty Analysis

The precision of the results acquired throughout the engine assessment procedure significantly influences the results section. The investigation cannot be finalized due to the delay caused by erroneous data or the existence of atmospheric anomalies during the testing stage. Consequently, an individual iteration method for data calibration and the calibration of certain experimental results yields a greater degree of ineffective outcomes. Conducting up to four assessments is recommended to minimize errors. Table 5 represents instruments utilized and the uncertainty that occurred during testing. Table 6

represents test parameters uncertainty. Reduced deviations yield a greater level of granularity in contrast with atmospheric anomalies and calibrated information. The difference in deviations subjected to actual data and calibrated data is scientifically expressed by the equation (1) referred from [24]

$$\sum R_{i=} \frac{2\sigma_r}{\bar{c}_{ni}} *100\text{-----(1)}$$

Ri = Initial readings that calibrated concerning atmospheric defects

From the Gaussian deviation of data, the actual readings are calibrated and defined by the deviations as represented in equation (2) referred from [25]

$$R_i = f(c_1, c_2, c_3, \_\_\_\_\_ c_n)\text{---------(2)}$$

σ_r = Deviation in calibrations during testing

$c_1, c_2, c_3,$ = Calibrated data during the measure of uncertainty

Table 5. Instruments Utilized and Uncertainties

SNO	Description	Range	Accuracy	uncertainty
1	Loading indicator	0–100 kg	±2.2 kg	0.22
2	Tachometer	0–11000 rpm	±8 rpm	0.12
3	Exhaust gas Temperature	0–900 °C	±1.1 °C	0.13
4	Manometer	0–220 mm	±2.1 mm	1.12
5	Smoke meter	0-11 BSU	±0.13	1.1
6	Crank angle Coder	250–420 deg	±1.1 deg	0.14
7	Stopwatch	–	±0.6s	0.22

Table 6. Test Parameters uncertainties

SNO	Parameter	Units	Percentage uncertainty
1	Airflow	Kg/s	±0.23
2	BTE	%	±0.06
3	BSFC	Kg/kWh	±0.08

4	HC	%	±11
5	CO_2	%	±0.12%
6	CO	%	±0.13%
7	NOx	ppm	±10
8	Smoke meter	%	±0.11

RESULTS AND DISCUSSION

Effects of Hydrogen On Performance

Brake thermal efficiency

The engine's performance is contingent upon the quantity of chemical energy released during the crankshaft's rotation to achieve brake power. Brake thermal efficiency is analytically defined as the ratio of braking power to the product of fuel mass and its calorific value necessary for heat liberation [26]. Figure 3 illustrates the brake thermal efficiency achieved by hydrogen and pyrolysis blends functioning in dual modes. Figure 3 a represents Experimental results, 3b represents RSM contour plots, 3 c represents 3-dimensional plots and 3 d represents predicted vs actual values. The 90D10P blend is specifically acknowledged for achieving a maximum brake thermal efficiency of 34%, but for diesel is 27.2%, The 90D10P exceeding diesel by 20%. This fuel's superior calorific value results in enhanced brake thermal efficiency compared to other mixes. Adjacent to the 90D10P, the 90D10P+50 LPH demonstrates enhanced brake thermal efficiency followed by 30%, which is 9.3% higher than diesel. Consequently, a blend of 90D10P achieves superior braking energy efficiency relative to diesel, attributable to its efficient comprehensive utilization, lightweight functioning, and diminished loss of warmth [27]. The incorporation hydrogen gas at a rate of 50 litres per hour enhances the ignition quality of combustion, resulting in superior brake thermal efficiency compared to diesel. The oxygen–air mixture along with the supercharged decomposition oil/diesel mixture (90D10P+50 LPH) promotes a greater oxidizing of the two elements species. This reduces hydrocarbons that and dust (minimizing chemical compounds loss), hence

enhancing the proportion of energy from combustibility converted into machinery. [28,29].

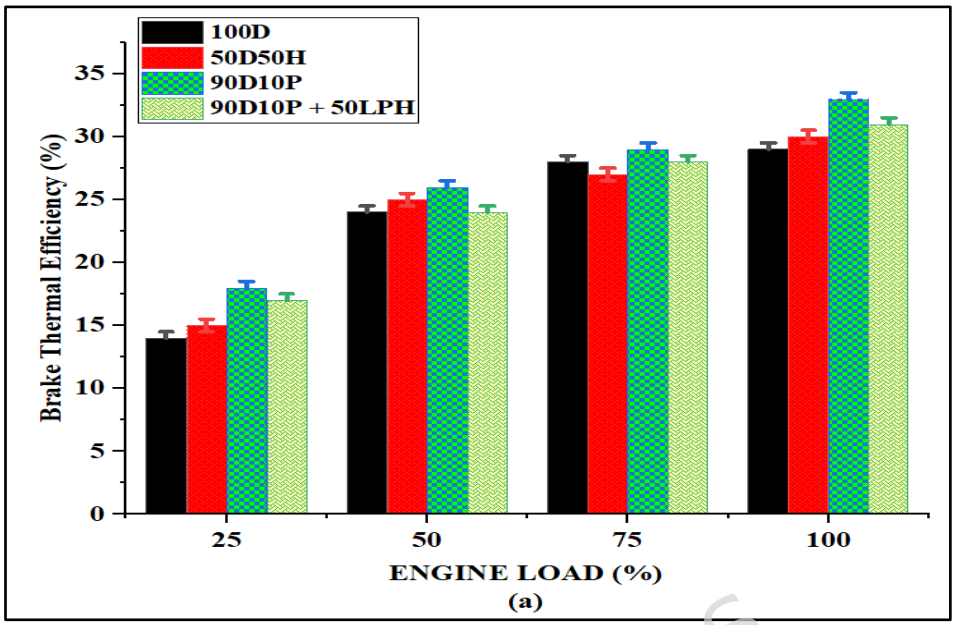

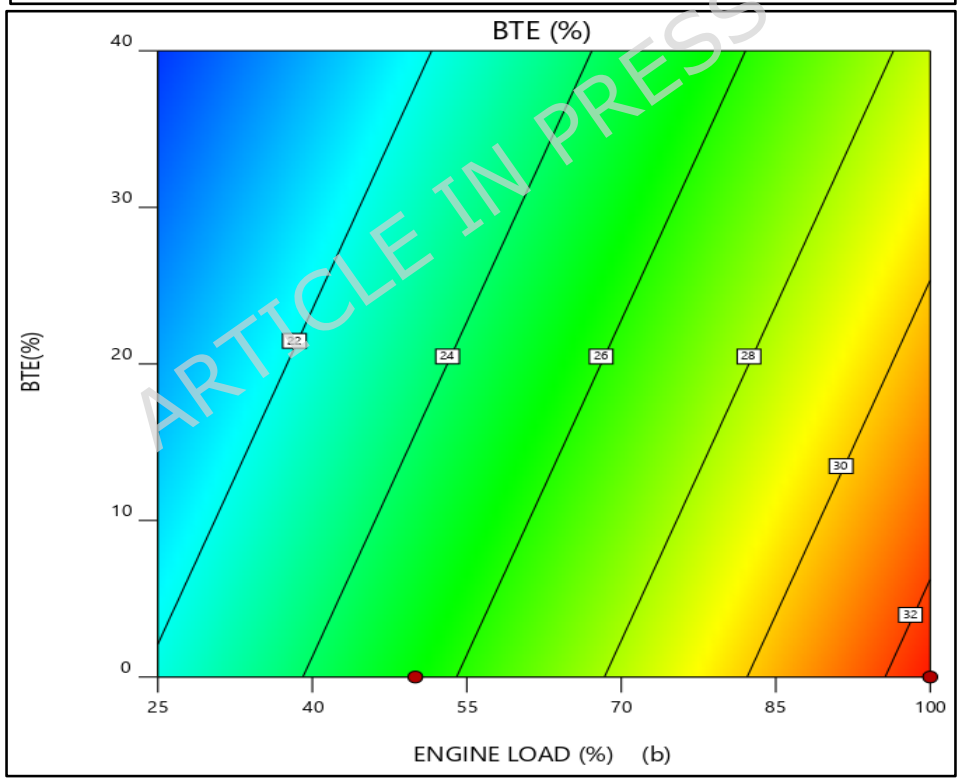

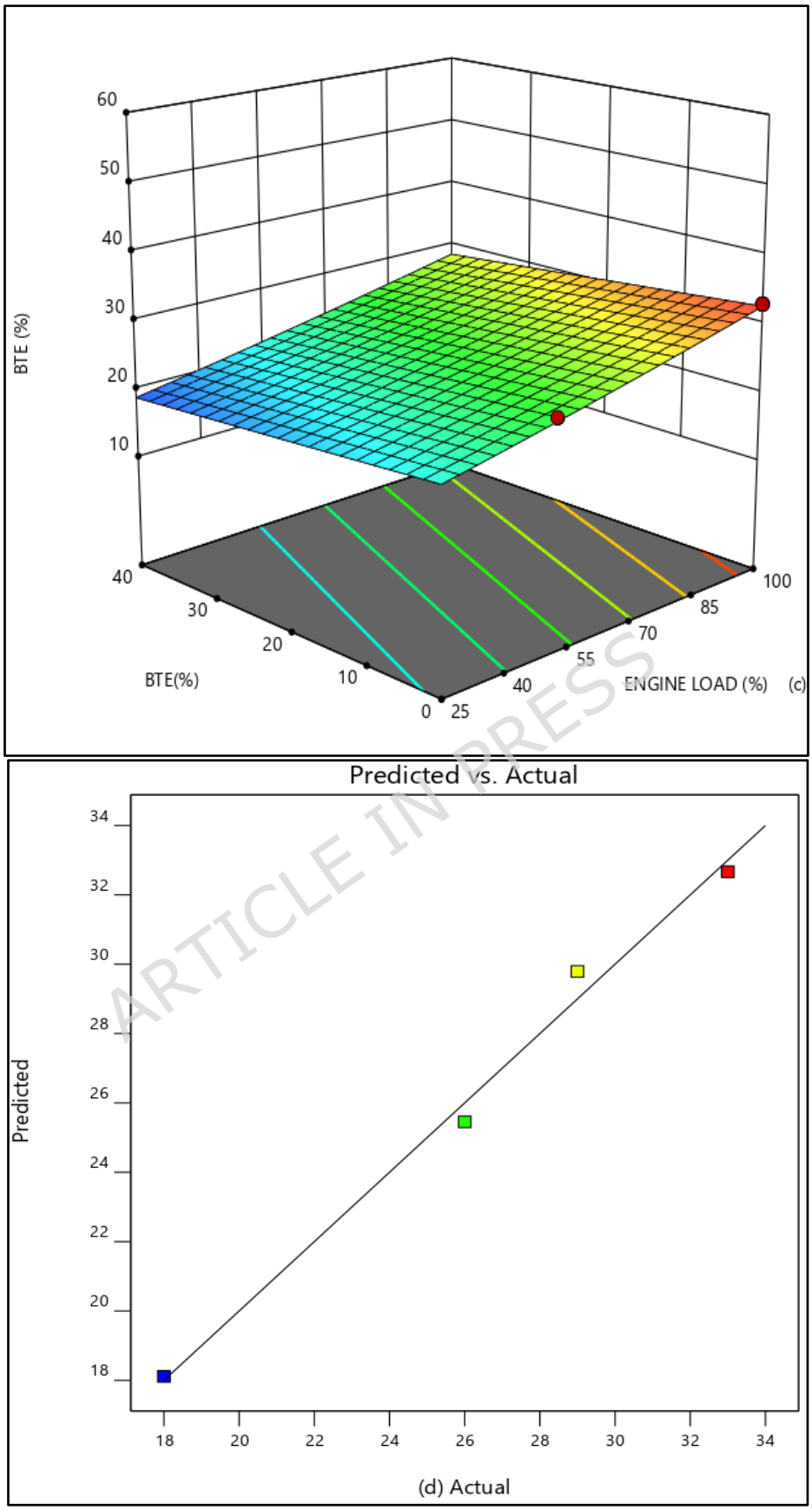

Figure 3. BTE a) Experimental b) Rsm Plots c) 3D Contour d) Predicted Vs Actual

The model's F value of 65.96 indicates an 8.67% probability that such a big F-value may arise from random variation. P-values below 0.0500 signify the significance of model terms. In this instance, there are no substantial model terms. Values beyond 0.1000 signify that the model terms lack significance. Model reduction may enhance your model if numerous inconsequential terms are present, except those necessary for hierarchy support. Table 7 illustrates the ANOVA findings for the BTE levels parameter. Table 8 illustrates the fit statistics of BTE models.

Table 7. Annova models for BTE

Origin	Summation	df	Square Root	F-prob	P-Prob	
Model	1.22	2	0.6107	65.96	0.0867	not significant
A-A	0.2324	1	0.2324	25.10	0.1254	
B-B	0.0732	1	0.0732	7.91	0.2175	
Remaining	0.0093	1	0.0093			
Total Cor	1.23	3				

Table 8. Fit Statics

Description	Value	RMS	Values
Devn.	0.0962	R^2	0.9925
Imply	5.12	Modified R^2	0.9774
CV %	1.88	Expected R^2	0.4320
		Precision	17.5162

The Estimated R^2 of 0.4320 significantly diverges from the adjusting R^2 of 0.9774, with a discrepancy over 0.2, which is atypical. This may suggest a significant block influence or a potential issue with the framework and/or data. Considerations include model decrease, response transformation, outliers, and others. All empirical models have to receive validation through confirmation runs.

Brake specific fuel consumption

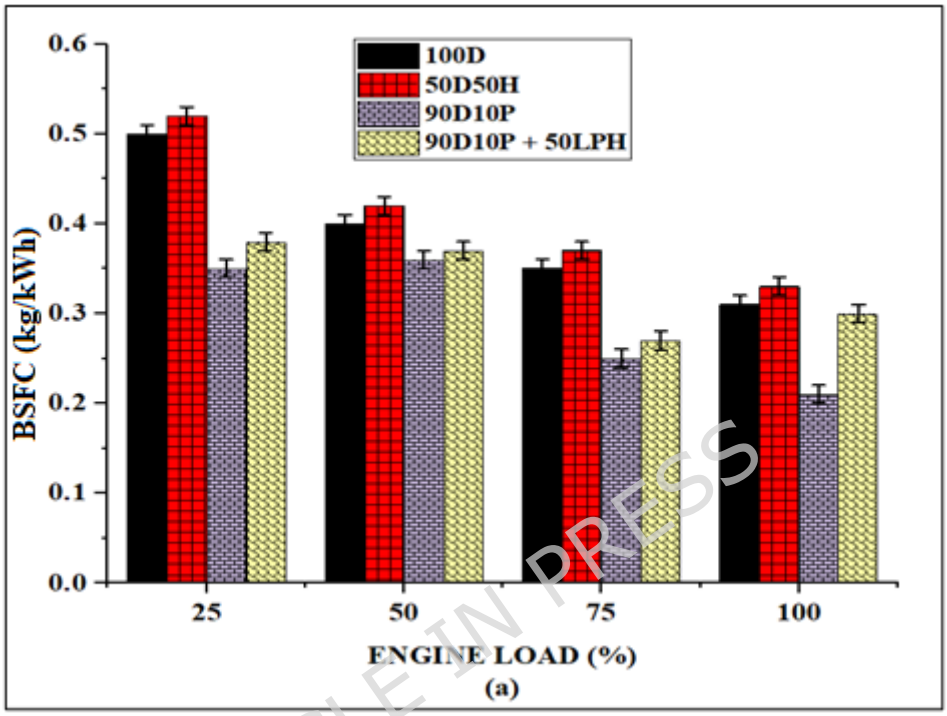

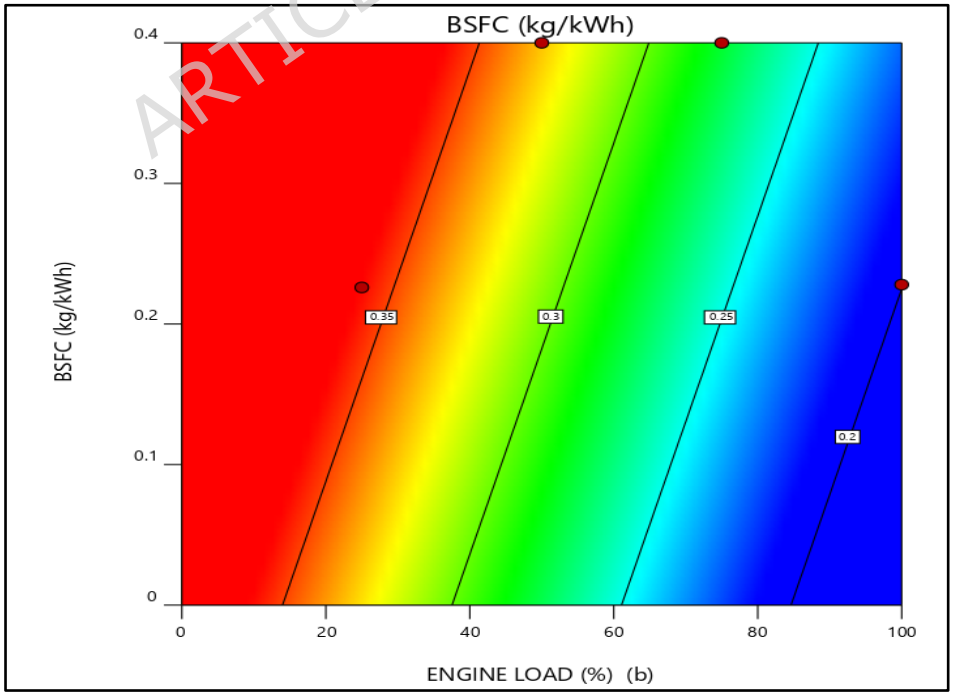

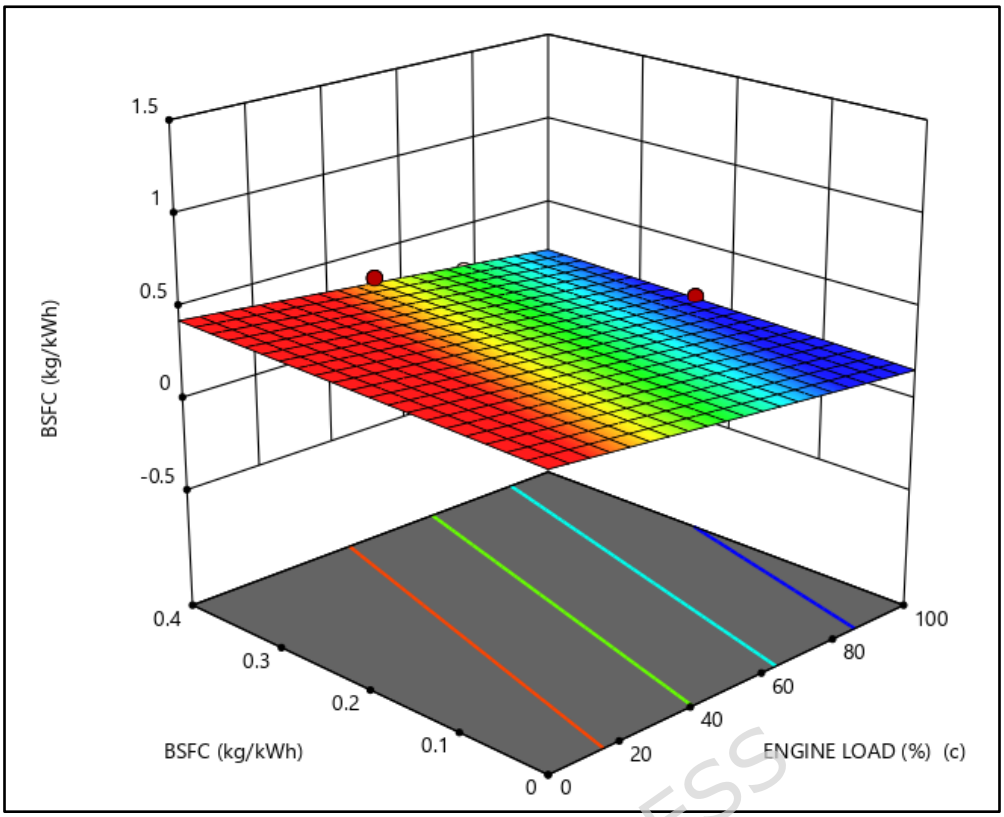

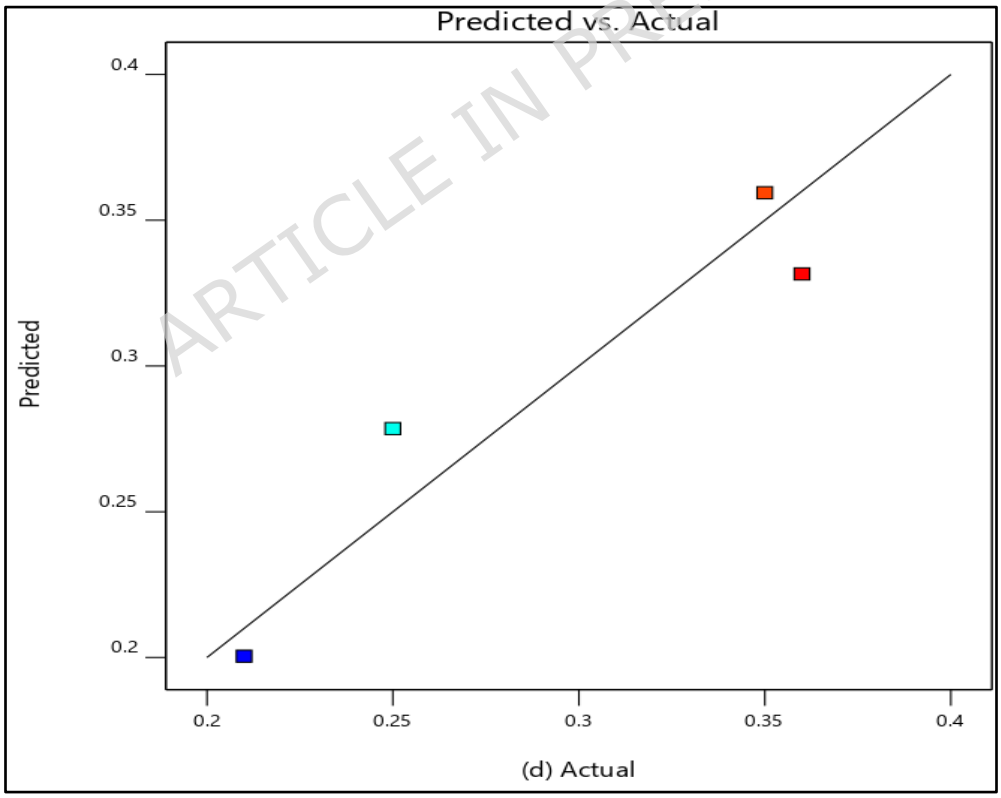

Figure 4. BSFC a) Experimental b) Rsm Plots c) 3D Contour d) Actual vs Predicted

The utilization of more fuel owing to the different load conditions subjected to lean and rich mixtures is technically defined by the parameter called specific fuel consumption [30,31]. The lower tends to higher the attainment at peak loads and the higher the specific fuel consumption leads to lower thermal efficiency, which the performance parameters [32]. Figure 4 technically explains the consumption of fuels owing to different load conditions subjected to experimental, RSM plots, contour plots and predicted values. From the figure, it is clearly understood that the 90D10P blend possesses minimal fuel consumption at peak loads. The attained consumption is found to be 0.22 kg/kWh, but for diesel, the consumption of attainment is found to be 0.35 kg/kWh.

The least consumption is attained for the fuel 90D10P and 90D10P +50 LPH blend than diesel. The addition of limited pyrolysis oil on diesel has potential benefits in terms of better oxidation capability to atomise the blends for achieving better combustion [33]. Also, Hydrogen strongly proved that it acts as a quenching blend which shortens the length of the flame owing to the mixing of 90D10P with 50 LPH accelerates the combustion efficiency with short intervals and achieves better consumption than diesel [34,35]. The enrichment of hydrogen gas premixing with biodiesel blends improves the consumption rate than diesel. The self-ignition temperature of hydrogen gas is better than biodiesel blends and this self-ignition temperature of hydrogen gas mixing with 90D10P followed by 50 LPH atomises the fuel better way to achieve the very least consumption than diesel [36,37].

The model's F value of 4.08 indicates appears insignificant. owing to magnitudes random variation is 33.05%. P probes less than 0.0501 signify that statistically good. In this instance, no substantial parameters. probs beyond 0.1000 signify that the predicted terms lack significance. The reductions of different types of probes, except those necessary for hierarchical support. Table 9 illustrates the ANOVA model for specific fuel usage.

Table 9. Annova Model of BSFC

Origin	Summation	df	Square Root	F-prob	P-Prob	
Model	0.0147	2	0.0073	4.08	0.3305	not significant
A-A	0.0141	1	0.0141	7.83	0.2185	
B-B	0.0006	1	0.0006	0.3504	0.6598	
Remaining	0.0018	1	0.0018			
Total Cor	0.0165	3				

Table 10. Fit Statics of BSFC

Description	Value	RMS	Values
Devn.	0.0424	R^2	0.8908
Imply	0.2925	Modified R^2	0.6723
CV %	14.50	Expected R^2	-3.8550
		Precision	4.3272

The predicted R^2 indicates, as illustrated in the preceding table, that the general average might serve as a superior predictor of your answer compared to the existing model. In certain instances, a more complex model may yield superior predictions. Adeq Precision quantifies the ratio of noise to signal. A ratio over 4 is preferable. Your proportion of 4.327 signifies a satisfactory indication. This paradigm may facilitate navigation inside the design space. Table 10 illustrates the fit data of Brake specific fuel consumption.

Effects of Hydrogen on Combustion

Inline Cylinder Pressures

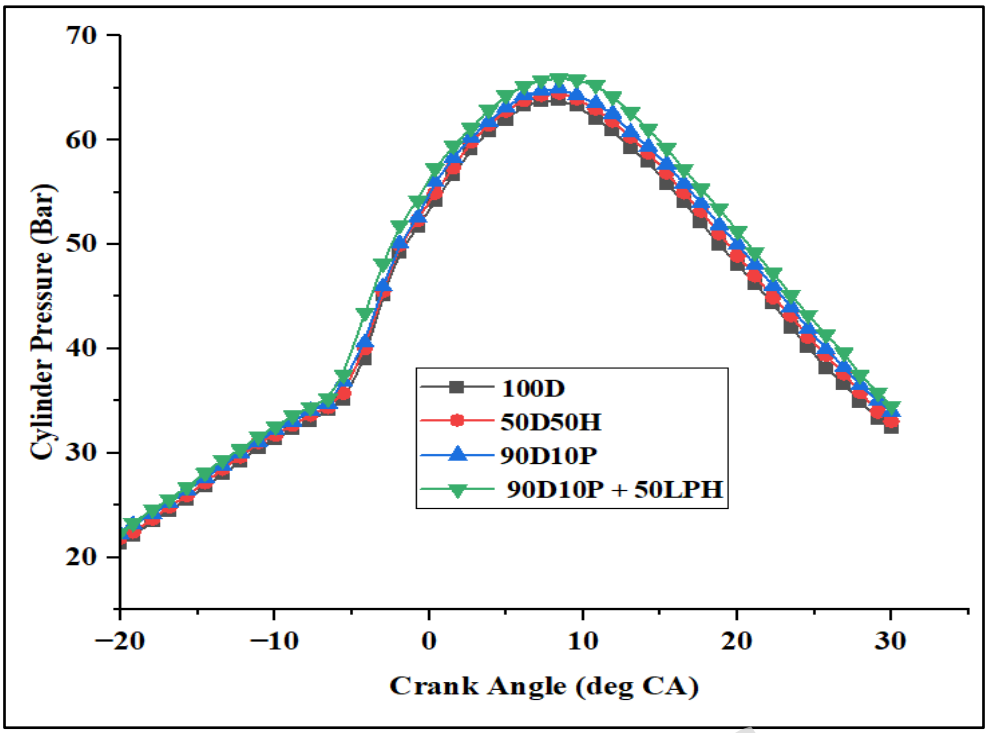

Figure 5. Inline cylinder pressures

The combustion phase is a very important phase which describes the attainment of heat release rates and the development of pressures that are attained inside the cylinder [38]. In other words, in-line cylinder pressure denotes the pressure produced within the burning cylinder of an engine with internal combustion [39]. Monitoring and studying this pressure are essential for comprehending the combustibility process and its effect on engine performance [40,41]. Figure 5 predominantly describes the inline cylinder pressures developed inside the combustion phase evolved by these four test fuels. At full load conditions concerned to 1500 rpm, the highest cylinder pressures is attained for the 90D10P + 50 LPH of 69 bar. But for the diesel the attained cylinder pressures are 60 bar. The fuel 90D10P + 50 LPH achieves 13.1% higher than diesel. The reason behind these blends for attaining the highest peak pressures subjected to different crank angles is the hydrogen gas acts as a carrier gas which adequate mixing of 90D10P with 50 LPH at shorter intervals with flame propagation speeds tends to attain higher surface tensions inside the combustion chamber causes highest inline cylinder pressures than diesel [42,43]. Every test were performed under identical cylinder

velocity, compression number, and load circumstances. The braking mean effectiveness resistance measurements were derived from the recorded braking intensity. The findings demonstrate that BMEP exhibited only slight fluctuations across the evaluated fuels. Minor decreases in Brake Mean Effective Pressure were noted for discarded plastic oil and its mixtures, mostly attributable to the diminished warmth and increased thickness, which can impair combustion performance.

The 90D10P blend comprises 10% leftover plastic oil, characterized by el evated fragrant amounts and an extended delayed ignition relative to die sel.This results in an increased mixes fuels proportion, leading to a heigh tened maximum temperature release throughout the mixed firestorm pha se.The diminished growth of flames and instability of discarded plastic oil hinder the accumulation of cylindrical tension, resulting in a maximum p ressure relative to diesel.The introduction of hydrogen (50 LPH) with 90 D10P markedly alters the way it burns kinetics.The hydrogen gas exhibits an exceptionally fast burn velocity, little burning lag, and extensive explo sive duration, facilitating swift burning upon burning.This results in an ac celerated and more pronounced tension increase, culminating in elevated peak pressures in the cylinder.Nonetheless, due to hydrogen's facilitatio n of converting from mixup to diffused burning, the mixup warming rate peak is diminishedthe conflagration transpires more rapidly and during a briefer period, leading to a decreased seeming HRR despite the total po wer released being comparable.

Heat Release Rates

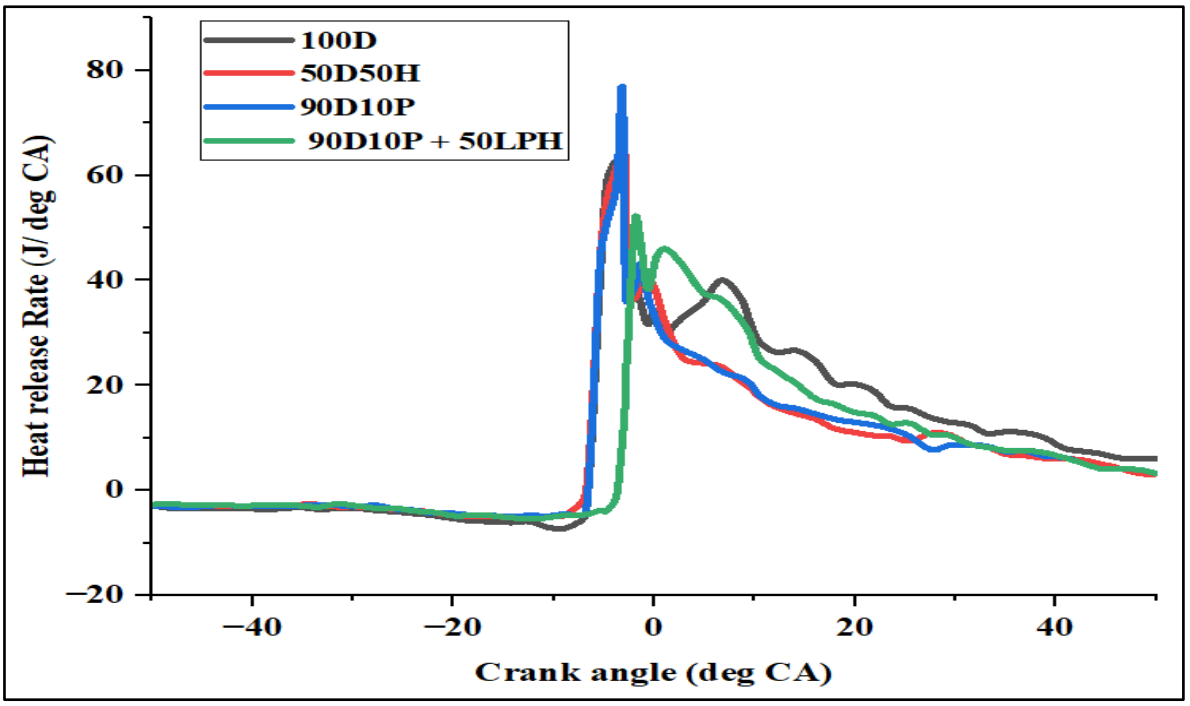

Figure 6. Heat release Rate

The heat release rate of a piston engine is characterized as the quantity of heat energy emitted per unit of time during combustion [44]. It is a significant metric for assessing the effectiveness of combustion, flaming stability, and contaminant deposition in engines. The rate of heat dissipation can influence the development of pollutants such as noble gases and aerosols (PM). Enhancing heat release rates can mitigate these emissions [45].

Theproper oversight of HRR helps avert engine knock, an aberration in w hich the fuel and air conjunction ignite early, triggering engine malfunctions [46]. Figure 6 deliberately explains about the test results obtained by the heat release rates of testing blends and diesel. Figure 6 demonstrates that the 90D10P and 90D10P + 50 LPH test fuels emit elevated heat rates of 78 J/deg CA and 75 J/deg CA, respectively. The superior oxidation stability provided by the two blends, 90D10P and 90D10P + 50 LPH, facilitates the management of thermal stress on the engine, reducing the likelihood of overheating and ensuring consistent performance, attributable to the enhanced surface tensions exhibited by these test fuels in comparison to diesel [47,48].In

terms of the overall heat release, both 90D10P and 90D10P + 50 LPH demonstrate somewhat reduced total heat release relative to pure diesel, attributable to the diminished calorific value associated with discarded plastic oil. The hydrogen-enriched mix (90D10P + 50 LPH) demonstrates superior combustibility, as the fast degradation of the hydrogen improves the utilization of energy and minimizes unburned hydrocarbons inefficiencies. The contrasting trajectories of maximal cylinders warmth and pressure release rate are ascribed to the transition in combustible mode from a primarily mixing phase (in 90D10P) to a simpler and rapid ignition (in 90D10P + 50 LPH) owing to the substance's enhanced combustible rates [49].

Effects of Hydrogen on Emissions

Carbon monoxide

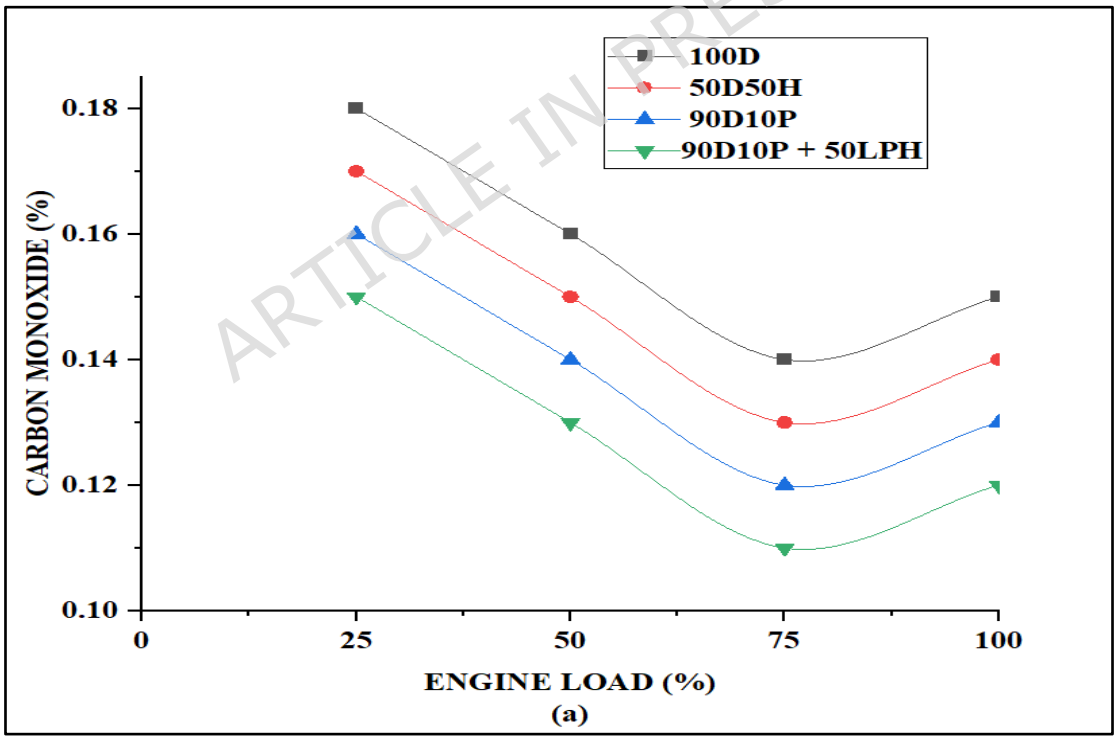

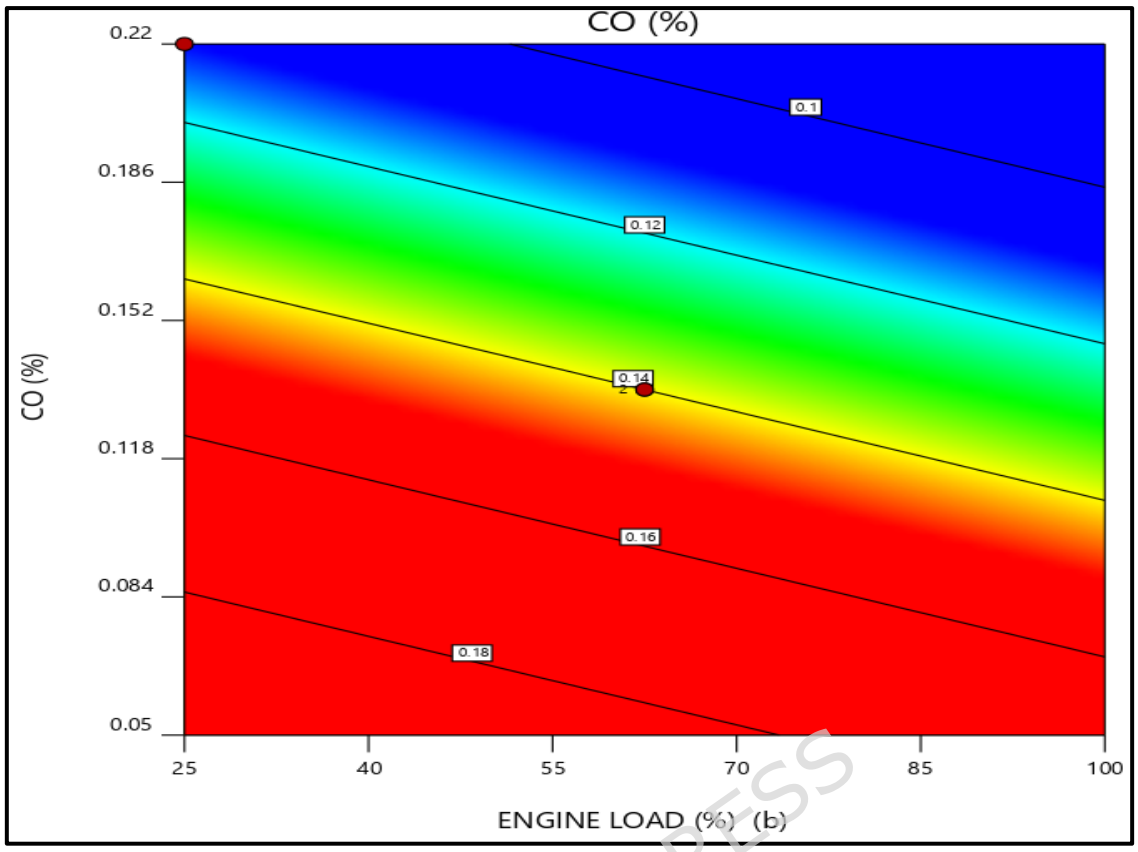

(b)

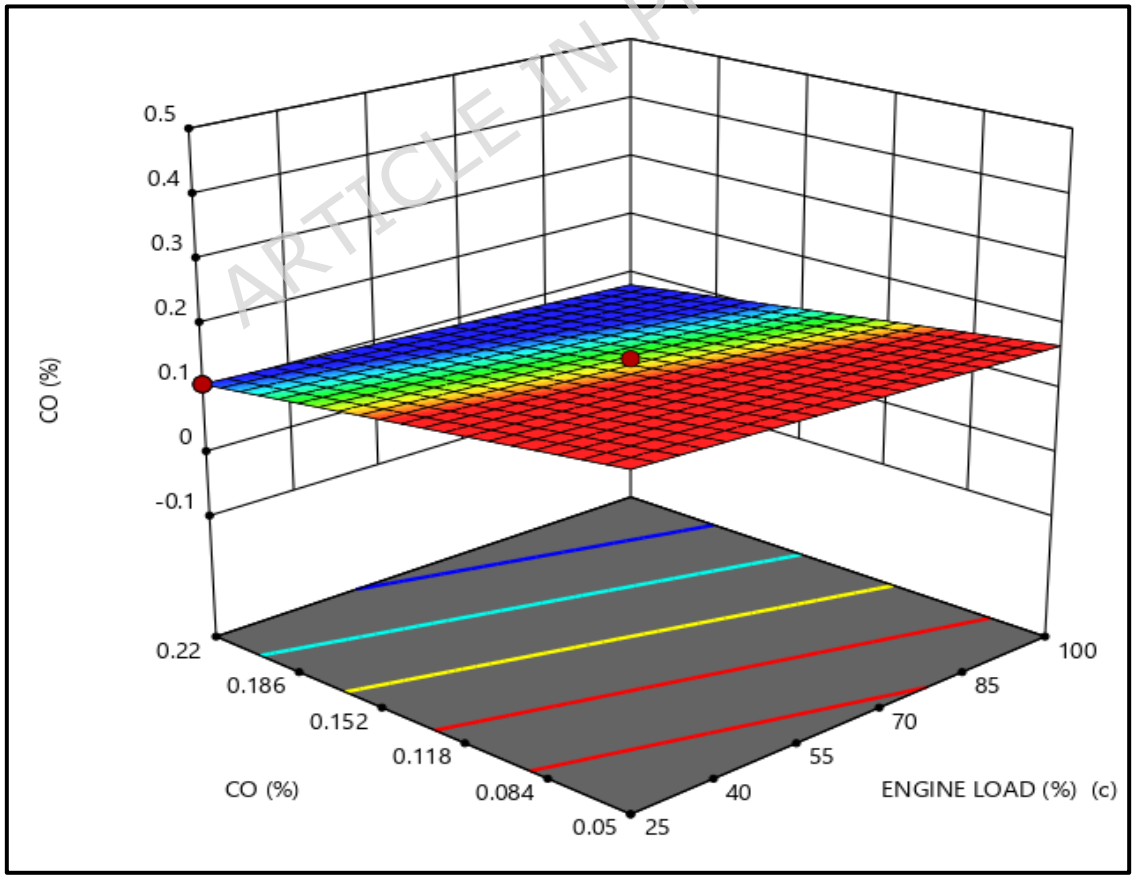

(c)

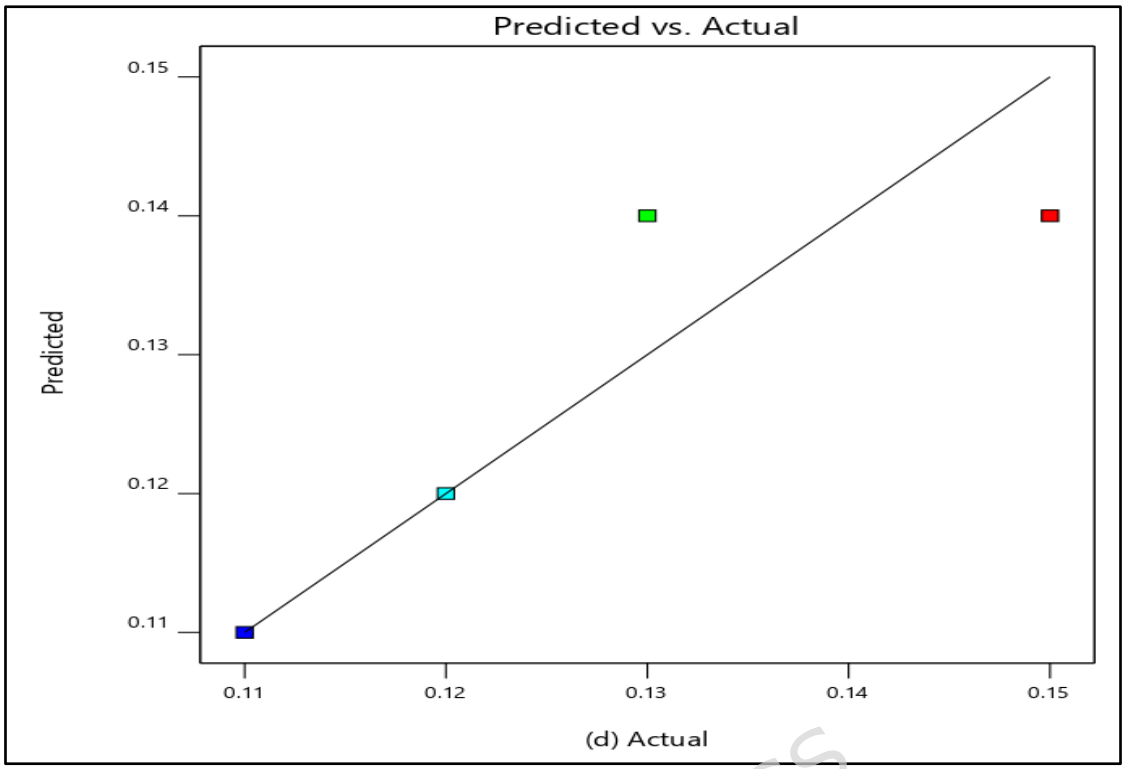

Figure 7. CO Emissions a) Experimental b) RSM Plots c) 3D Contour d) Predicted vs Actual

The Major factors that contribute to the release of toxic gases include automobiles and other forms of equipment that rely on petroleum or natural gas to power their operations. These emissions are the result of the slow-burning of air with fuel. . Carbon monoxide is a harmless gas that has the prospective to harm both humans and the environment. It is colourless and odourless. Inhaling carbon monoxide, a poisonous gas, can lead to major health complications [50]. Symptoms such as vertigo, weakness, nausea, disorientation, and loss of consciousness can occur after a short period of treatment. The initial. Heart disease, decreased oxygen supply to tissues, and neurological damage are all possible outcomes of excessive exposure [51]. Figure 7 deliberately explains the formation of CO particles owing to different parameters concerning experimental, RSM, 3D and predicted values. From Figure 7, it is significantly proved that the least possible emissions are achieved for both fuels concerning 90D10P and 90D10P + 50 LPH blends. Comparatively very least emissions are formed for the fuel and 90D10P + 50 LPH followed

by 0.13%, but for pure diesel 0.17%, The 90D10P + 50 LPH attains lowest CO by 30.7%. because of very short ignition delay and lower viscosity for limited 10P, pyrolysis oil oxidises with hydrogen gas very quickly and releases the CO particles very low than diesel and other blends [52,53].

The model's F value of 1.69 indicates that the predicted value is insignificant in comparison to the chaos. The probability of obtaining an F-value of this magnitude owing to random variations. P-values below 0.0500 signify that model terms are statistically significant. In this instance, there are no substantial model terms. Values beyond 0.1000 signify that the model terms lack significance. Model reduction may enhance the structure of your model if numerous irrelevant terms are present (excluding those necessary to maintain hierarchy). Adeq Precision quantifies the ratio of signals to noise. A ratio of 2.45 signifies an insufficient signal and complicates navigation within the design space. Annova results of CO are shown in Table 11 and fit statistics are represented in Table 12.

Table 11 Annova for CO Models

Origin	Summation	df	Square Root	F-prob	P-Prob	
Model	0.0007	2	0.0003	1.69	0.4781	not significant
A-A	0.0003	1	0.0003	1.33	0.4544	
B-B	0.0007	1	0.0007	3.29	0.3206	
Remaining	0.0002	1	0.0002			
Total Cor	0.0009	3				

Table 12. Fit statistics for CO models

Description	Value	RMS	Values
Devn.	0.0141	R^2	0.7714
Imply	0.1275	Modified R^2	0.3143
CV %	11.09	Expected R^2	NA
		Precision	2.4495

Carbon dioxide

Carbon dioxide discharges from diesel engines denote the discharge of CO_2 gas into the natural environment as a consequence of combustion [54].

The incomplete combustion of carbon atoms with oxygen atoms owing to different temperatures and different pressures results in combustion fuel by combining it with air, resulting in a chemical reaction that generates energy, in the form of carbon dioxide [55]. This gas exacerbates warming temperatures and results in climate challenges across the world [56]. Figure 8 deliberately explains the formation of carbon dioxide emissions in the form of particulate matter released by diesel and test fuels. From the figure 8 it is significantly proved that minimum formation of carbon dioxide emissions is achieved for the 90D10P + 50 LPH followed by 7%, but for diesel CO_2 emissions are 9%. The decrease in emissions for 90D10P + 50 LPH is 28.5% than diesel. This is due to the phenomenon of higher oxidation stability of hydrogen gas equipped with limited pyrolysis oil and diesel. This turns to oxidise well at the precombustion stage and dissipates the heat very smoother and faster than other test blends. Better oxidation of hydrogen gas with 90D10P followed by 50 LPH results in the minute formation of CO_2 particles [57, 58].

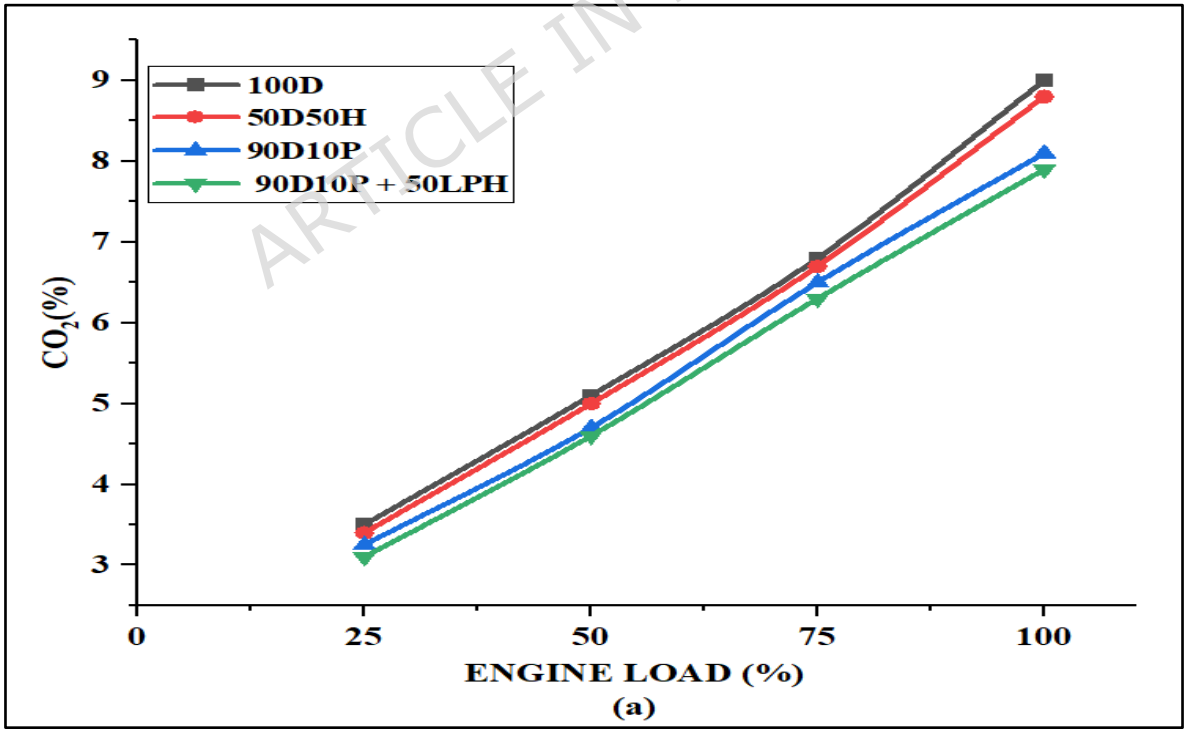

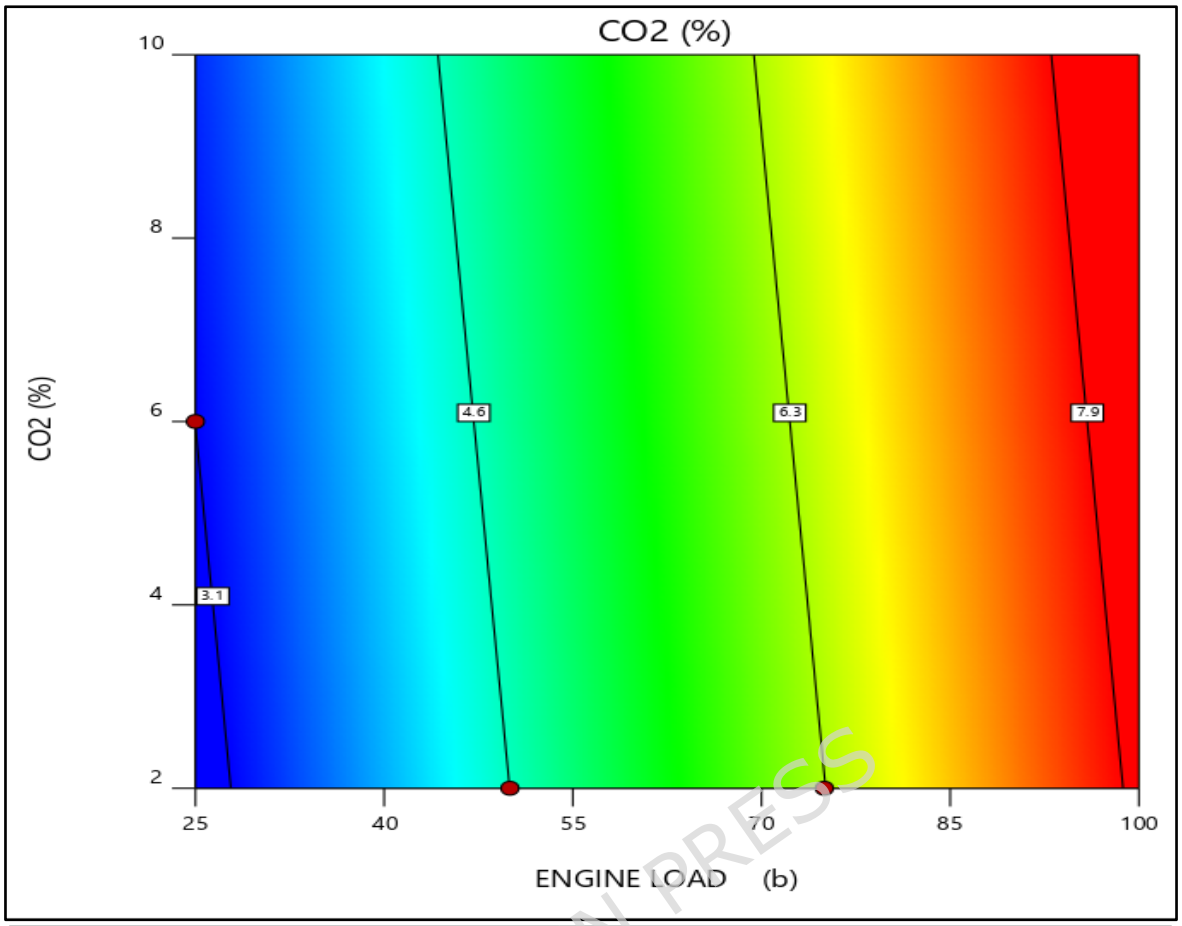

(b)

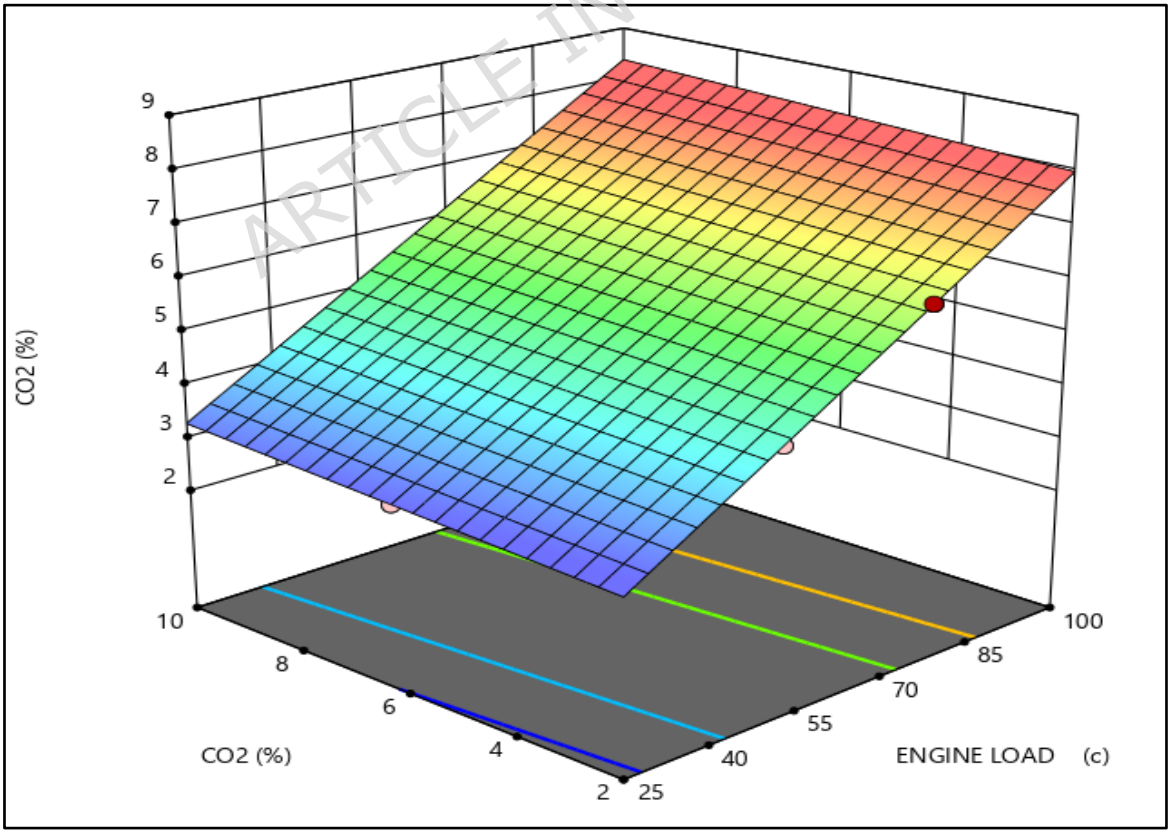

(c)

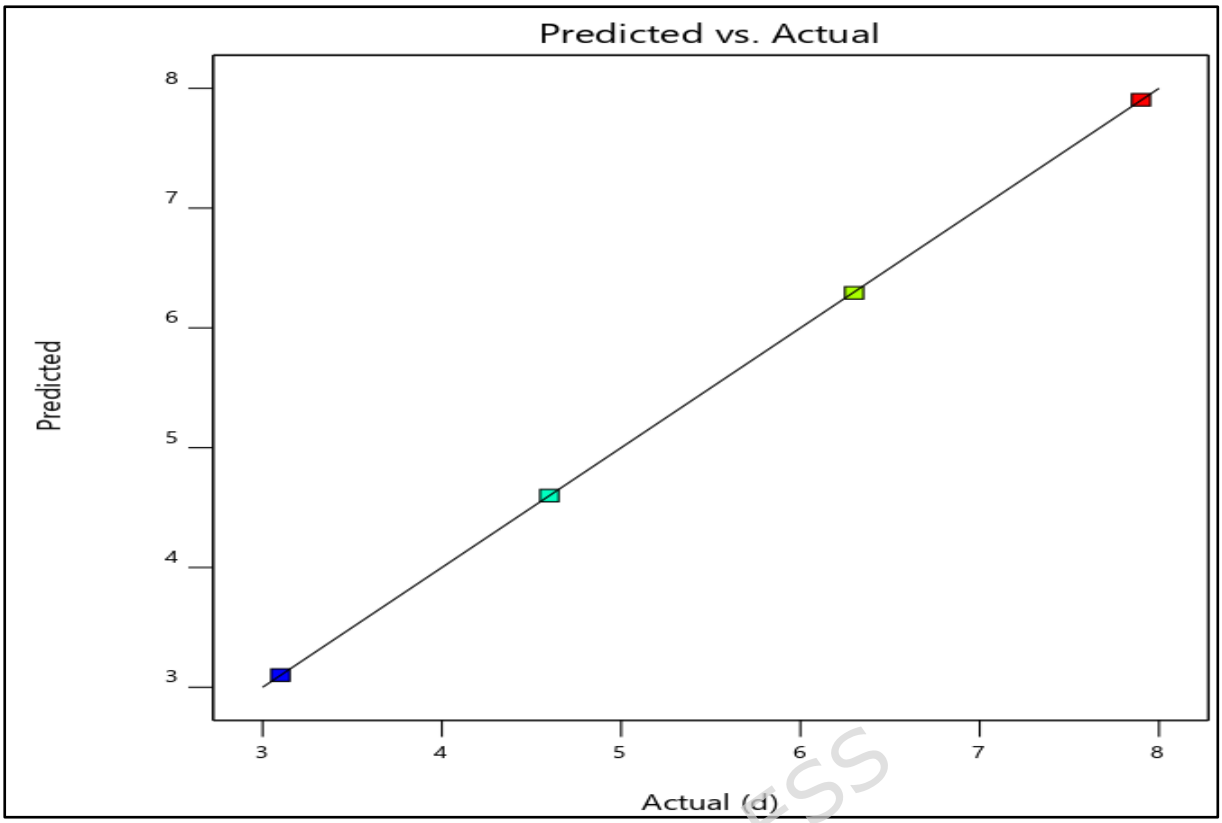

Figure 8.CO_2 Emissions a) Experimental b) RSM Plots c) 3D Contour d) Predicted vs actual

The model's F-value of 81840.89 indicates that the model seems significant. The probability of an F-value of this magnitude arising from random noise is about 0.25%. P-values below 0.0500 signify the significance of model terms. A constitutes a substantial model word. Values beyond 0.1000 signify that the model terms lack significance. Model reduction may enhance the CO2 model if numerous inconsequential terms are included, except those necessary for hierarchy support. Table 10 illustrates ANOVA models of CO_2 formations. Table 13 represents Annova results for CO_2 models and its fit statistics is represented in Table 14.

Table 13. Annova for CO_2 models

Origin	Summation	df	Square Root	F-prob	P-Prob	
Model	12.97	2	6.48	81840.89	0.0025	Significant
A-A	2.45	1	2.45	30912.08	0.0036	

B-B	0.0069	1	0.0069	87.36	0.0679
Remaining	0.0001	1	0.0001		
Total Cor	12.97	3			

Table 14. Fit Statistics of CO_2 models

Description	Value	RMS	Values
Devn.	0.0089	R^2	1.0000
Imply	5.47	Modified R^2	1.0000
CV %	0.1626	Expected R^2	0.9991
		Precision	623.0582

The Expected R^2 of 0.9991 aligns well with the Calculated R^2 of 1.0000, with a difference of less than 0.2. Adeq Precision quantifies the signal-to-noise ratio. A ratio over 4 is preferable. The proportion of 623.058 signifies a satisfactory signal. This paradigm can facilitate navigation inside the design space.

Hydrocarbons

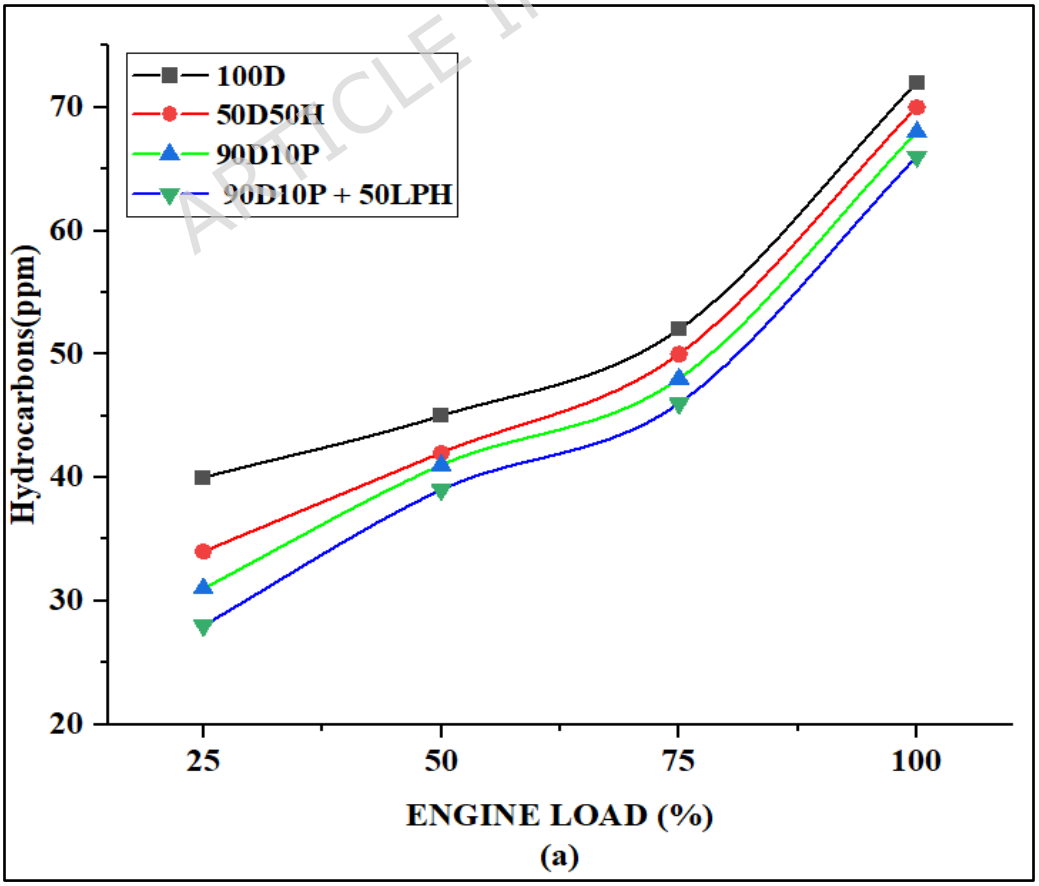

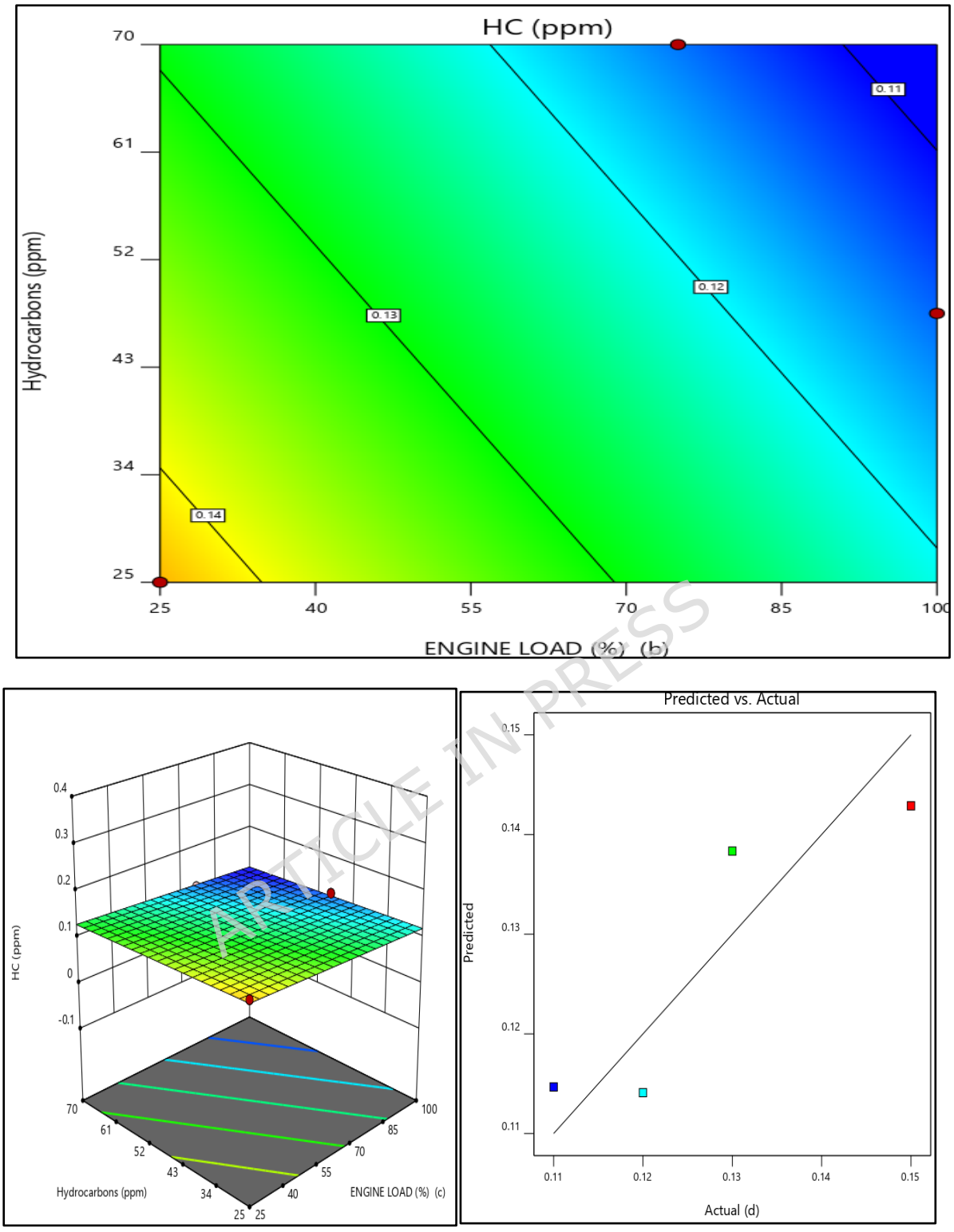

Figure 9. HC Emissions a) Experimental b) RSM Plots c) 3D Contour d) predicted vs actual

Hydrocarbon (HC) pollutants from diesel engines denote the discharge of unburned or imperfectly combusted fuel through the atmosphere [59]. These emissions arise from incomplete combustion, frequently attributable to issues such as inadequate engine adjustment, cold starts, or deficient air-fuel ratios [60]. Hydrocarbon emissions facilitate the development of ambient ozone and smog and can, therefore, adversely affect people's health and the environment [61]. Figure 9 describes the amount of Hydrocarbon emissions released to the atmosphere in terms of experimental results, RSM plots, 3D Contour and predicted values. From the figure, it is understood that compared to pure diesel 100 D, the very least HC emissions are achieved for the test blends 90D10P and 90D10P + 50 LPH in the range of 63 ppm for the fuel 90D10P + 50 LPH and 66 ppm for the blend 90D10P, but for the pure diesel the attained HC emissions were 73 ppm. The HC emissions is low for 90D10P + 50 LPH, which is 10.6% less than diesel. The reason behind the HC emissions for the fuel 90D10P + 50 LPH being very low because that hydrogen gas acts as a superior oxidation stability during the mixing of pyrolysis oil with diesel owing to limit the carbon molecules during combustion tends to form a lean mixture and achieves very less emissions compared to diesel [62,63]. One more reason for achieving very low emissions for the fuel 90D10P + 50 LPH is hydrogen career gas acts as a superior blend in terms of combustion of hydrogen generates higher temperatures than that of diesel or biodiesel fuels. Consequently, augmenting biodiesel/diesel fuels with hydrogen enhances the reduced Hydrocarbon levels. Notably, these alterations in HC emissions align with the caloric value of biofuel and Hydrogen gas[64]. The hydrocarbon emissions diminished with the utilization of Hydrogen gas, contributing to the enhanced integration of hydrogen and air, accelerated burning, and increased flame diffusion [65]. The oxygen in Hydrogen gas facilitates the full ignition of biodiesel and diesel [66]. Table 15 represents Annova for HC Models.

The model's F-value of 1.97 indicates that the predicted value is insignificant in comparison to the noise. The probability of an F-value of this magnitude arising from random variation is 44.97%. P-values below

0.0500 signify that the model terms are statistically significant. In this instance, there are no substantial model terms. Values beyond 0.1000 signify that the model terms lack significance. Model reduction may enhance your model if numerous inconsequential terms are present, except those necessary for hierarchy support. A disadvantage The predicted R^2 suggests that the average of all variables could serve as a superior predictor of your answer compared to the existing model. In certain instances, a higher-order structure may yield superior predictions. Adeq Precision quantifies the signal-to-noise ratio. A coefficient of 2.50 signifies an insufficient signal, and this model should not be utilized for navigating the design area. Table 16 illustrates the fit estimates for HC models.

Table 15. Annova for HC Models

Origin	Summation	df	Square Root	F-prob	P-Prob	
Model	0.0007	2	0.0003	1.97	0.4497	not significant
A-A	0.0002	1	0.0002	0.8844	0.5195	
B-B	0.0001	1	0.0001	0.5257	0.6006	
Remaining	0.0002	1	0.0002			
Total Cor	0.0009	3				

Table 16. Fit Statistics of HC models

Description	Value	RMS	Values
Devn.	0.0133	R^2	0.7978
Imply	0.1275	Modified R^2	0.3933
CV %	10.43	Expected R^2	2.8848
		Precision	2.4981

Nitrogen Oxides

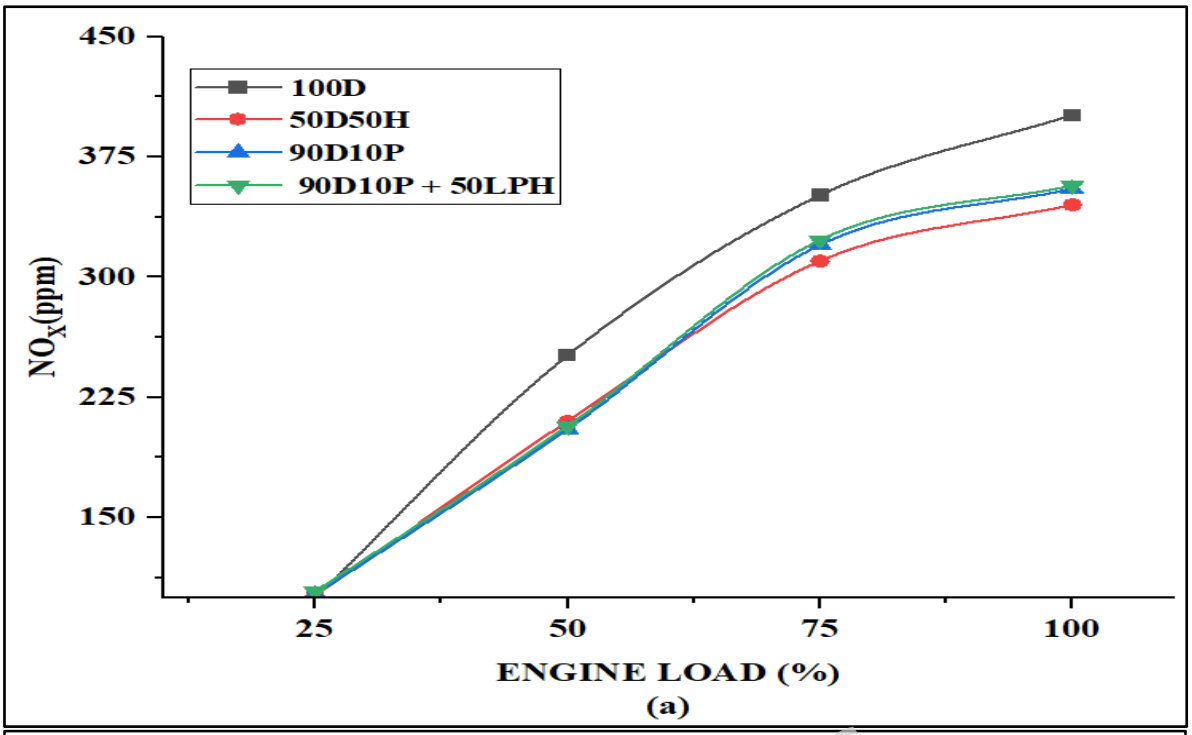

(a)

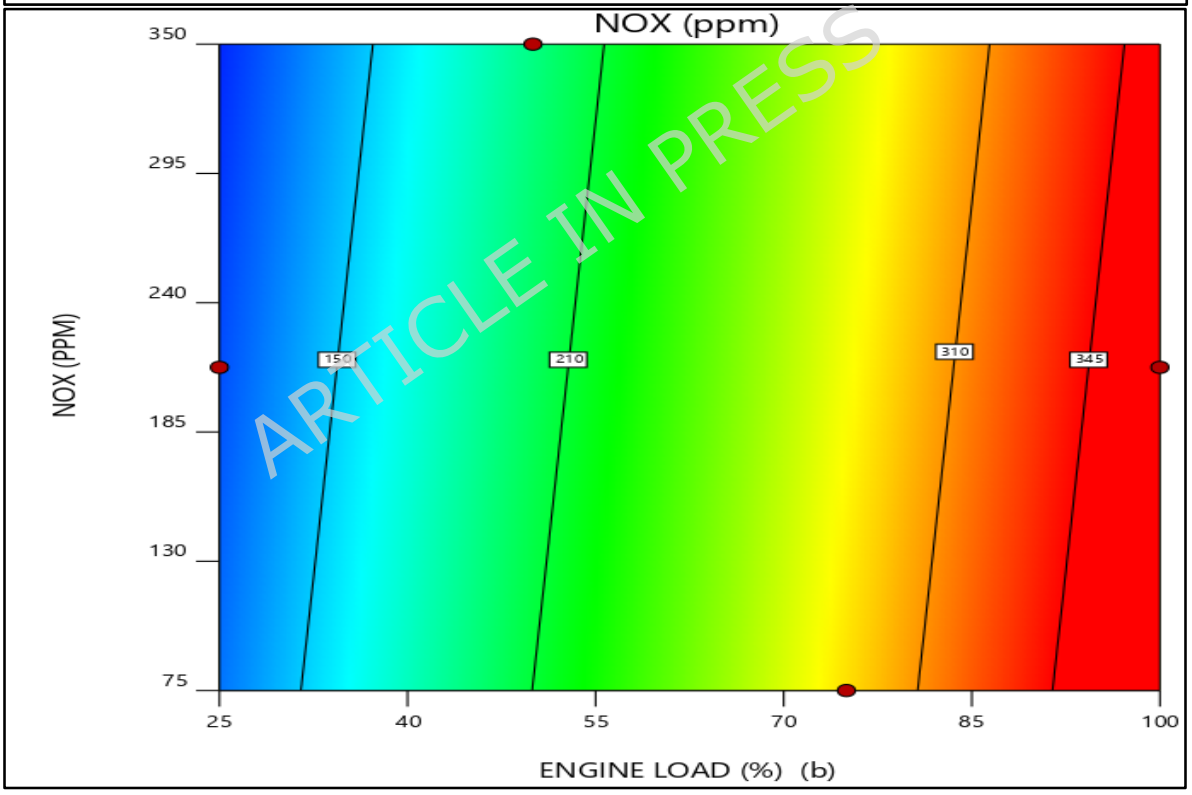

(b)

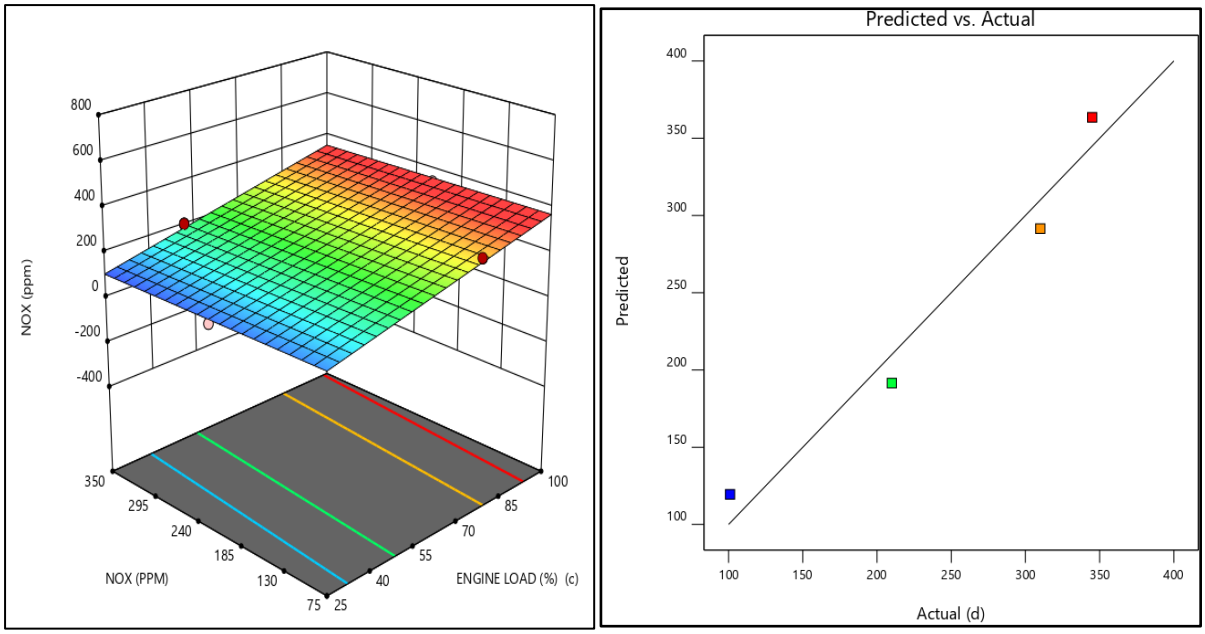

Figure 10. NO_X Emissions a) Experimental b) RSM Plots c) 3D Contour d) predicted vs actual

Nitrogen-oxygen (NOx) that emanates from diesel engines denote the discharge of nitrogen oxides, chiefly the pollutants nitric oxide (NO) and dioxide of nitrogen (NOx), into the environment as a consequence of combustion [67]. These emissions arise from increased temperatures and elevations in diesel engines, leading to the reaction of nitrogen in the air with oxygen, resulting in the formation of NOx gaseous substances [68]. Figure 10 represents the formations of NO_X subjected to experimental, RSM, 3D and predicted values. From Figure 10, it is deliberately understood that the formation of NO_X is very low for the test blend with an equivalent mass of hydrogen gas with an equivalent mass of diesel, Because at peak loads the higher the formation of temperature leads to inadequate proportions of hydrogen gas with pyrolysis oil and diesel results in incomplete combustion results in formations of higher NO_X for the blends 90D10P, and 90D10P+50 LPH and diesel than 50D50H. 50D50H possess very low NOx followed by 350 ppm, but for diesel NO_X emits 400 ppm. Which NO_X for fuel 50D50H is 14.2% less than diesel. Another reason for getting very NOx particulates for the blend 50D50H is shorter the ignition delay occurs for this test fuel, because basically, diesel is a highly oxygenated fuel [69], When it oxidised with hydrogen gas at elevated temperatures results in quicker burning of nitrogen molecules

with oxygen molecules tending to achieve the combustion faster and faster with complete combustions followed by least particulates [70,71].50D50H attains very Lowest NOX compared to other blends, because Reduced Mean Combustion Temperature The generation of NO_x (nitrogen oxides) adheres to the thermodynamic (Zeldovich) cycle, which escalates significantly when flame values surpass around 1800 K.In a dual-energy configuration of 50H–50P (pyrolysis of hydrogen into oil):The element hydrogen combusts rapidly yet can be well regulated (lean combustion with surplus air).This type of oil comprises oxidized molecules and typically exhibits a lower calorie density, resulting in a reduced cumulative heating rate compared to diesel fuel at equivalent loads. The combination is often thinner, distributing the flame and diminishing localized hot spots. The oxygenated composition of the pyrolysis oil (50D50H) diminishes affluent regions. This kind of oil is abundant in oxygenation compounds, including spirits, ketones, benzene, and acidity. This facilitates deeper degradation of fuel molecules, especially in cooler regions. It also diminishes concentrated fuelled regions that generate extremely hot homogeneous domains conducive to NO_x formation during diesel burning. Burning becomes evenly distributed and colder, resulting in a reduction in oxides of nitrogen[72]. The model's F value of 12.70 indicates that the predicted value is insignificant in comparison to the noise. The probability of attaining an F-value of this magnitude due to random variation is 19.46%. P-values below 0.0500 signify that the model terms are statistically significant. In this instance, there are no substantial model terms. Values beyond 0.1000 signify that the model terms lack significance. Model reduction may enhance the NO_X model if numerous inconsequential terms are present, except those necessary for hierarchical support. Table 17 illustrates the ANOVA for NO_X models. Table 18 represents Fit statistics of NO_X models[73].

The anticipated R^2 of 0.3939 is not in proximity to the Modified R^2 of 0.8863, with a discrepancy over 0.2. This may suggest a significant barrier effect or a potential issue with your framework and/or data. Considerations

include model reduction, response modification, outliers, and others. All empirical models must undergo validation through confirmation runs.

Table 17. Annova for NO_X models

Origin	Summation	df	Square Root	F-prob	P-Prob	
Model	34768.00	2	17384.00	12.70	0.1946	not significant
A-A	29768.00	1	29768.00	21.74	0.1345	
B-B	156.80	1	156.80	0.1145	0.7923	
Remaining	1369.00	1	1369.00			
Total Cor	36137.00	3				

Table 18. Fit statistics of NO_X models

Description	Value	RMS	Values
Devn.	37.00	R^2	0.9621
Imply	241.50	Modified R^2	0.8863
CV %	15.32	Expected R^2	0.3939
		Precision	7.6148

CONCLUSION

The studies examine the performance of a diesel engine working in dual mode using the test fuels 100D, 50D50H, 90D10P, and 90D10P + 50 LPH. The performance, combustion, and emission characteristics of a diesel engine fuelled with a blend of gaseous hydrogen and pyrolysis oils mixed with diesel are enhanced by specific percentages, attributable to the advantages of hydrogen gas in facilitating smoother combustion, as evidenced by the rate of heat release and inline the cylinder pressures. Moreover, the minimal emission characteristics are generated by the heat release associated with the amalgamation of pyrolysis fuel and diesel operating at 50 LPH enriched gas. The results of the experiment are juxtaposed with RSM charts related to both 2D and 3D representations. The linear aggressiveness model most accurately fits all loads, followed by performance, combustion, and emission factors. The ANOVA technique provides a concise assessment of the model's performance, indicating that

the experimental results closely align with the obtained parameters. The subsequent results were obtained during the experimental procedure.

- The 90D10P mixture is deliberately acknowledged for achieving optimal braking thermal efficiency of 34%, exceeding diesel by 21.4%. The fuel's elevated energy density leads to improved brake thermal efficiency relative to other mixtures.
- The 90D10P blend exhibits minimal fuel usage under peak loads. The achieved consumption is 0.22 kg/kWh, whereas the average utilization for diesel is 0.35 kg/kWh. The lowest consumption is achieved with the 90D10P fuel compared to diesel, due to its superior oxidation rate and enhanced evaporation process.
- 90D10P + 50 LPH fuel possesses the highest inline cylinder pressure of 69 bar. The reason behind these blends for attaining the highest peak pressures subjected to different crank angles is the hydrogen gas acts as a carrier gas to attain minimum flame propagations.
- 90D10P and 90D10P + 50 LPH test fuels release high heat rates followed by 78 J /deg CA and 75 J /deg CA. The good oxidation stability offered by these two blends 90D10P and 90D10P + 50 LPH aids with regulating the thermal burden on the engine, mitigating the risk of scorching.
- The very least emissions are formed for the fuel and 90D10P + 50 LPH followed by 0.13%, but for pure diesel 0.17%, The 90D10P + 50 LPH attains lowest CO by 30.7%. because of very short ignition delay and lower viscosity for limited 10P, pyrolysis oil oxidises with hydrogen gas very quickly and releases the CO particles very low than diesel and other blends.
- The minimum formation of carbon dioxide emissions is achieved for the 90D10P + 50 LPH followed by 7%, but for diesel CO_2 emissions are 9%. The decrease in emissions for 90D10P + 50 LPH is 28.5% than diesel. This is due to the phenomenon of higher oxidation stability of hydrogen gas equipped with limited pyrolysis oil and diesel.

- The very least HC emissions are achieved for the test blends 90D10P and 90D10P + 50 LPH in the range of 63 ppm for the fuel 90D10P + 50 LPH and 66 ppm for the blend 90D10P, but for the pure diesel the attained HC emissions were 73 ppm. The HC emissions is low for 90D10P + 50 LPH, which is 10.6% less than diesel.
- 50D50H possess very low NOx followed by 350 ppm, but for diesel NOX emits 400 ppm. Which NOX for fuel 50D50H is 14.2% less than diesel. Another reason for getting very NOx particulates for the blend 50D50H is shorter the ignition delay occurs for this test fuel, because basically, diesel is a highly oxygenated fuel.
- 50D50H attains very Lowest NO_X compared to other blends, because reduced mean combustion temperature is attained for this 50D50H. The generation of NO_x (nitrogen oxides) adheres to the thermodynamic (Zeldovich) cycle, which escalates significantly when flame values surpass around 1800 K.In a dual-energy configuration of 50H–50P (pyrolysis of hydrogen into oil):The element hydrogen combusts rapidly yet can be well regulated (lean combustion with surplus air).This type of oil comprises oxidized molecules and typically exhibits a lower calorie density, resulting in a reduced cumulative heating rate compared to diesel fuel at equivalent loads. The combination is often thinner, distributing the flame and diminishing localized hot spots.
- The oxygenated composition of the pyrolysis oil (50D50H) diminishes affluent regions. This kind of oil is abundant in oxygenation compounds, including spirits, ketones, benzene, and acidity. This facilitates deeper degradation of fuel molecules, especially in cooler regions. It also diminishes concentrated fuelled regions that generate extremely hot homogeneous domains conducive to NO_x formation during diesel burning. Burning becomes evenly distributed and colder, resulting in a reduction in oxides of nitrogen.

NOMENCLATURE

ANOVA – Analysis of Variance

BTE – Brake Thermal Efficiency
B10 – 10% Biodiesel+90% diesel
B15 -15% Biodiesel+85% diesel
BSFC-Brake Specific fuel consumption
EGR – Exhaust gas recirculation.
BDC- Bottom dead centre
TDC- Top dead centre
HC – Hydrocarbons
CO – Carbon monoxide
CI -Compression Ignition
CA- Crank Angle
CRDI - Common Rail Direct Injection
CO_2 – Carbon dioxide
DI – Direct ignition
NO_X – Nitrogen oxides
HRR- Heat release rate
HHO – Hydroxy gas
H_2 – Hydrogen gas
LPH – Litres per hour
LPM – Litres per minute
LDPE – Low-density polyethylene
HDPE – High-density polyethylene
PET – Polyethylene terephthalate
PVC- Polyvinyl chloride
RSM – Response surface methodology
100D- 100% diesel
50D50H -50% diesel+50% hydrogen gas
90D10P -90% diesel + 10% pyrolysis oil
2D – 2 dimensional
3D – 3 Dimensional

Declarations

Conflict interests

"The authors declare that they have no conflict of interest."

Data Availability: The data that supports the findings of this study are available within the article.

Funding: The authors extend their appreciation to the Deanship of Research and Graduate Studies at King Khalid University for funding this work through Large Research Project under grant number RGP2/491/46.

Author Contribution Statement: Conceptualization, K.S.K; Writing—Review and Editing, K.S.K, R.S; Formal analysis, M.K, S.K; Investigation, A.I.A.A, A.F.E.

Acknowledgement:

The authors extend their appreciation to the Deanship of Research and Graduate Studies at King Khalid University for funding this work through Large Research Project under grant number RGP2/491/46.

REFERENCES

1. Kanth, S. and Debbarma, S., 2021. Comparative performance analysis of diesel engine fuelled with hydrogen-enriched edible and non-edible biodiesel. International Journal of Hydrogen Energy, 46(17), pp.10478-10493.
2. Zhang, X., Yang, R., Anburajan, P., Van Le, Q., Alsehli, M., Xia, C. and Brindhadevi, K., 2022. Assessment of hydrogen and nanoparticles blended biodiesel on the diesel engine performance and emission characteristics. Fuel, 307, p.121780.
3. Çalık, A., 2018. Determination of vibration characteristics of a compression ignition engine operated by hydrogen-enriched diesel and biodiesel fuels. Fuel, 230, pp.355-358.
4. Ramalingam, S., DhakshinaMoorthy, M. and Subramanian, S., 2022. Effect of natural antioxidant additive on hydrogen-enriched biodiesel operated compression ignition engine. International Journal of Hydrogen Energy, 47(48), pp.20771-20783.

5. Elnajjar, E., Al-Omari, S.A.B., Selim, M.Y.E. and Purayil, S.T.P., 2022. CI engine performance and emissions with waste cooking oil biodiesel boosted with hydrogen supplement under different load and engine parameters. Alexandria Engineering Journal, 61(6), pp.4793-4805.
6. Akcay, M., Yilmaz, I.T. and Feyzioglu, A., 2020. Effect of hydrogen addition on performance and emission characteristics of a common-rail CI engine fueled with diesel/waste cooking oil biodiesel blends. Energy, 212, p.118538.
7. Chaurasiya, P.K., Rajak, U., Veza, I., Verma, T.N. and Ağbulut, Ü., 2022. Influence of injection timing on performance, combustion and emission characteristics of a diesel engine running on hydrogen-diethyl ether, n-butanol and biodiesel blends. International Journal of Hydrogen Energy, 47(41), pp.18182-18193.
8. Jamrozik, A., 2025. An Overview of Development and Challenges in the Use of Hydrogen as a Fuel for a Dual-Fuel Diesel Engine. Energies, 18(21), p.5793.
9. Hosseini, S.H., Tsolakis, A., Alagumalai, A., Mahian, O., Lam, S.S., Pan, J., Peng, W., Tabatabaei, M. and Aghbashlo, M., 2023. Use of hydrogen in dual-fuel diesel engines. Progress in Energy and Combustion Science, 98, p.101100..
10. Estrada, L., Moreno, E., Gonzalez-Quiroga, A., Bula, A. and Duarte-Forero, J., 2022. Experimental assessment of performance and emissions for hydrogen-diesel dual fuel operation in a low displacement compression ignition engine. Heliyon, 8(4).
11. Panait, A., Pana, C., Cernat, A., Negurescu, N., Nutu, C., Fuiorescu, D. and Nemoianu, L., 2025. The Use of Hydrogen in the Automotive Diesel Engine—An Efficient Solution to Control Its Operation with Reduced Carbon Emissions. Sustainability, 17(22), p.10369.
12. Akhtar, M.U.S., Asfand, F., Khan, M.I., Mishra, R. and Ball, A.D., 2025. Performance and emissions characteristics of hydrogen-

diesel dual-fuel combustion for heavy-duty engines. International Journal of Hydrogen Energy.

13. Tan, D., Wu, Y., Lv, J., Li, J., Ou, X., Meng, Y., Lan, G., Chen, Y. and Zhang, Z., 2023. Performance optimization of a diesel engine fueled with hydrogen/biodiesel with water addition based on the response surface methodology. Energy, 263, p.125869.
14. Wang, Y., Sedghi, R., Shahbeik, H., Hosseinzadeh-Bandbafha, H., Pan, J., Tabatabaei, M. and Aghbashlo, M., 2024. A comprehensive review of exergy analysis in biodiesel-powered engines for sustainable power generation. Sustainable Energy Technologies and Assessments, 68, p.103869.
15. Thiyagarajan, S., Varuvel, E., Karthikeyan, V., Sonthalia, A., Kumar, G., Saravanan, C.G., Dhinesh, B. and Pugazhendhi, A., 2022. Effect of hydrogen on compression-ignition (CI) engine fueled with vegetable oil/biodiesel from various feedstocks: A review. International Journal of Hydrogen Energy, 47(88), pp.37648-37667.
16. Pullagura, G., Vanthala, V.S.P., Vadapalli, S., Bikkavolu, J.R., Barik, D., Sharma, P. and Bora, B.J., 2024. Enhancing performance characteristics of biodiesel-alcohol/diesel blends with hydrogen and graphene nanoplatelets in a diesel engine. International Journal of Hydrogen Energy, 50, pp.1020-1034.
17. Singh, K., Dwivedi, G., Verma, T.N. and Shukla, A.K., 2024. Energy, exergy, emissions and sustainability assessment of hydrogen supplemented diesel dual fuel turbocharged common rail direct injection diesel engine. International Journal of Hydrogen Energy.
18. Hosseini, S.H., Tsolakis, A., Alagumalai, A., Mahian, O., Lam, S.S., Pan, J., Peng, W., Tabatabaei, M. and Aghbashlo, M., 2023. Use of hydrogen in dual-fuel diesel engines. Progress in Energy and Combustion Science, 98, p.101100.
19. Rajpoot, A.S., Choudhary, T., Chelladurai, H.M. and Dwivedi, G., 2023. A novel comprehensive energy, exergy and sustainability

analysis of a diesel engine powered by binary blends of juliflora biodiesel and nanoparticles. Journal of Thermal Analysis and Calorimetry, 148(21), pp.11981-11997.

20. Algayyim, S.J.M., Saleh, K., Wandel, A.P., Fattah, I.M.R., Yusaf, T. and Alrazen, H.A., 2024. Influence of natural gas and hydrogen properties on internal combustion engine performance, combustion, and emissions: A review. Fuel, 362, p.130844.
21. Pachiannan, T., Zhong, W., He, Z., Alharbi, S.A. and Brindhadevi, K., 2025. Assessing the performance, and emissions characteristics of a diesel engine fueled with soya seed biodiesel blended with oxy-hydrogen. International Journal of Hydrogen Energy, 139, pp.1008-1014.
22. Bala Prasad, K., Meduri, O., Dhana Raju, V., Azmeera, A.K., Venu, H., Subramani, L. and Soudagar, M.E.M., 2025. Effect of split fuel injection strategies on the diverse characteristics of CRDI diesel engine operated with tamarind biodiesel. Energy Sources, Part A: Recovery, Utilization, and Environmental Effects, 47(1), pp.3566-3584.
23. Ramalingam, S., Rajkumar, T., Subramanian, S. and Palani, S., 2024. Investigation of combustion, emission, and performance parameters of a natural antioxidant additives using hydrogen and biodiesel as dual fuel in CI engine operation. International Journal of Hydrogen Energy, 110, pp.44-54.
24. Zhang, W., Wu, F., Luo, X., Song, L., Wang, X., Zhang, Y., Wu, J., Xiao, Z., Cao, F., Bi, X. and Feng, Y., 2024. Quantification of NOx sources contribution to ambient nitrate aerosol, uncertainty analysis and sensitivity analysis in a megacity. Science of The Total Environment, 926, p.171583.
25. Alruqi, M., Sharma, P., Deepanraj, B. and Shaik, F., 2023. Renewable energy approach towards powering the CI engine with ternary blends of algal biodiesel-diesel-diethyl ether: Bayesian optimized Gaussian process regression for modeling-optimization. Fuel, 334, p.126827.
26. Tan, D., Meng, Y., Tian, J., Zhang, C., Zhang, Z., Yang, G., Cui, S., Hu, J. and Zhao, Z., 2023. Utilization of renewable and sustainable diesel/methanol/n-butanol (DMB) blends for reducing

the engine emissions in a diesel engine with different pre-injection strategies. Energy, 269, p.126785.

27. Chen, J., Yu, H., Xu, H., Lv, Q., Zhu, Z., Chen, H., Zhao, F. and Yu, W., 2024. Investigation on Traffic Carbon Emission Factor Based on Sensitivity and Uncertainty Analysis. Energies, 17(7), p.1774.
28. Alrbai, M., Ahmad, A.D., Al-Dahidi, S., Abubaker, A.M., Al-Ghussain, L., Alahmer, A. and Akafuah, N.K., 2023. Performance and sensitivity analysis of raw biogas combustion under homogenous charge compression ignition conditions. Energy, 283, p.128486.
29. Winangun, K., Setiyawan, A. and Sudarmanta, B., 2023. The combustion characteristics and performance of a Diesel Dual-Fuel (DDF) engine fueled by palm oil biodiesel and hydrogen gas. Case Studies in Thermal Engineering, 42, p.102755.
30. Tüccar, G., 2021. Experimental study on vibration and noise characteristics of a diesel engine fueled with mustard oil biodiesel and hydrogen gas mixtures. Biofuels.
31. Thiyagarajan, S., Varuvel, E., Karthickeyan, V., Sonthalia, A., Kumar, G., Saravanan, C.G., Dhinesh, B. and Pugazhendhi, A., 2022. Effect of hydrogen on compression-ignition (CI) engine fueled with vegetable oil/biodiesel from various feedstocks: A review. International Journal of Hydrogen Energy, 47(88), pp.37648-37667.
32. Yin, Y., Medwell, P.R., Gee, A.J., Foo, K.K. and Dally, B.B., 2023. Fundamental insights into the effect of blending hydrogen flames with sooting biofuels. Fuel, 331, p.125618.
33. Wang, S., Zhang, Z., Hou, X., Lv, J., Lan, G., Yang, G. and Hu, J., 2023. The environmental potential of hydrogen addition as complementation for diesel and biodiesel: A comprehensive review and perspectives. Fuel, 342, p.127794.
34. Aydın, S., 2020. Comprehensive analysis of combustion, performance and emissions of power generator diesel engine fueled with different source of biodiesel blends. Energy, 205, p.118074.

35. Simsek, S. and Uslu, S., 2020. Experimental study of the performance and emissions characteristics of fusel oil/gasoline blends in spark ignited engine using response surface methodology. Fuel, 277, p.118182.

36. Kamarulzaman, M.K. and Abdullah, A., 2020. Multi-objective optimization of diesel engine performances and exhaust emissions characteristics of Hermetia illucens larvae oil-diesel fuel blends using response surface methodology. Energy Sources, Part A: Recovery, Utilization, and Environmental Effects, pp.1-14.

37. Kenanoğlu, R., Baltacıoğlu, M.K., Demir, M.H. and Özdemir, M.E., 2020. Performance & emission analysis of HHO enriched dual-fuelled diesel engine with artificial neural network prediction approaches. International Journal of Hydrogen Energy, 45(49), pp.26357-26369.

38. Baltacioglu, M.K., Arat, H.T., Özcanli, M. and Aydin, K., 2016. Experimental comparison of pure hydrogen and HHO (hydroxy) enriched biodiesel (B10) fuel in a commercial diesel engine. International Journal of Hydrogen Energy, 41(19), pp.8347-8353.

39. Elgarhi, I., El-Kassaby, M.M. and Eldrainy, Y.A., 2020. Enhancing compression ignition engine performance using biodiesel/diesel blends and HHO gas. International Journal of Hydrogen Energy, 45(46), pp.25409-25425.

40. Najafi, B., Haghighatshoar, F., Ardabili, S., S. Band, S., Chau, K.W. and Mosavi, A., 2021. Effects of low-level hydroxy as a gaseous additive on performance and emission characteristics of a dual fuel diesel engine fueled by diesel/biodiesel blends. Engineering Applications of Computational Fluid Mechanics, 15(1), pp.236-250.

41. Khan, M.B., Kazim, A.H., Farooq, M., Javed, K., Shabbir, A., Zahid, R., Fatima, S., Danish, M.R., Ali, Q., Chaudhry, I.A. and Atabani, A.E., 2021. Impact of HHO gas enrichment and high purity biodiesel on the performance of a 315 cc diesel engine. International Journal of Hydrogen Energy, 46(37), pp.19633-19644.

42. Subramanian, B., Lakshmaiya, N., Ramasamy, D. and Devarajan, Y., 2022. Detailed analysis on engine operating in dual fuel mode with different energy fractions of sustainable HHO gas. Environmental Progress & Sustainable Energy, 41(5), p.e13850.

43. Sudrajat, A., Tamaldin, N., Yamin, A.K.M., Bin, M.F., Tunggal, D. and Chichiri, B., 2020. Performance analysis of biodiesel engine by addition of HHO gas as a secondary fuel. Jurnal Tribologi, 26, pp.120-134.

44. Finesso, R. and Spessa, E., 2014. A real time zero-dimensional diagnostic model for the calculation of in-cylinder temperatures, HRR and nitrogen oxides in diesel engines. Energy Conversion and Management, 79, pp.498-510.

45. Mesa, E.S.C., Quintana, S.H. and Bedoya, I.D., 2024. Combustion stability, RGF and pressure referencing effect on HRR for a high compression ratio SI engine with natural gas lean mixtures. Case Studies in Thermal Engineering, 53, p.103891.

46. Li, W., Liu, Z., Wang, Z., Dou, H., Wang, C. and Li, J., 2016. Experimental and theoretical analysis of effects of equivalence ratio on mixture properties, combustion, thermal efficiency and exhaust emissions of a pilot-ignited NG engine at low loads. Fuel, 171, pp.125-135.

47. Chen, L., Wei, H., Pan, J., Liu, C. and Shu, G., 2020. Understanding the correlation between auto-ignition, heat release and knocking characteristics through optical engines with high compression ratio. Fuel, 261, p.116405.

48. Thangaraj, S. and Govindan, N., 2018. Evaluating combustion, performance and emission characteristics of diesel engine using karanja oil methyl ester biodiesel blends enriched with HHO gas. International Journal of Hydrogen Energy, 43(12), pp.6443-6455.

49. Ganesan, S., Thiruselvam, K. and Jayavelu, S., 2025. Towards green mobility: investigating hydrogen-enriched waste plastic

biodiesel blends with n-butanol for sustainable diesel engine applications. Energy Advances, 4(6), pp.763-775.

50. Dewangan, A., Mallick, A., Yadav, A.K., Islam, S., Saleel, C.A., Shaik, S. and Ağbulut, Ü., 2023. Production of oxy-hydrogen gas and the impact of its usability on CI engine combustion, performance, and emission behaviours. Energy, 278, p.127937.
51. Subramanian, B. and Thangavel, V., 2020. Experimental investigations on performance, emission and combustion characteristics of Diesel-Hydrogen and Diesel-HHO gas in a Dual fuel CI engine. International journal of hydrogen energy, 45(46), pp.25479-25492.
52. Demir, U., Çelebi, S. and Özer, S., 2024. Experimental investigation of the effect of fuel oil, graphene and HHO gas addition to diesel fuel on engine performance and exhaust emissions in a diesel engine. International Journal of Hydrogen Energy, 52, pp.1434-1446.
53. Gad, M.S. and Razek, S.A., 2021. Impact of HHO produced from dry and wet cell electrolyzers on diesel engine performance, emissions and combustion characteristics. International Journal of Hydrogen Energy, 46(43), pp.22277-22291.
54. Tsujimura, T. and Suzuki, Y., 2017. The utilization of hydrogen in hydrogen/diesel dual fuel engine. International journal of hydrogen energy, 42(19), pp.14019-14029.
55. Hosseini, S.M. and Ahmadi, R., 2017. Performance and emissions characteristics in the combustion of co-fuel diesel-hydrogen in a heavy duty engine. Applied Energy, 205, pp.911-925.
56. Dewangan, A., Mallick, A., Yadav, A.K., Islam, S., Saleel, C.A., Shaik, S. and Ağbulut, Ü., 2023. Production of oxy-hydrogen gas and the impact of its usability on CI engine combustion, performance, and emission behaviors. Energy, 278, p.127937.
57. Akal, D., Öztuna, S. and Büyükakın, M.K., 2020. A review of hydrogen usage in internal combustion engines (gasoline-Lpg-diesel)

from combustion performance aspect. International journal of hydrogen energy, 45(60), pp.35257-35268.

58. Alrazen, H.A., Talib, A.A., Adnan, R. and Ahmad, K.A., 2016. A review of the effect of hydrogen addition on the performance and emissions of the compression–Ignition engine. Renewable and Sustainable Energy Reviews, 54, pp.785-796.
59. Rosha, P., Kumar, S., Kumar, P.S., Kowthaman, C.N., Mohapatra, S.K. and Dhir, A., 2022. Impact of compression ratio on combustion behavior of hydrogen enriched biogas-diesel operated CI engine. Fuel, 310, p.122321.
60. Bakar, R.A., Kadirgama, K., Ramasamy, D., Yusaf, T., Kamarulzaman, M.K., Aslfattahi, N., Samylingam, L. and Alwayzy, S.H., 2022. Experimental analysis on the performance, combustion/emission characteristics of a DI diesel engine using hydrogen in dual fuel mode. International Journal of Hydrogen Energy.
61. Zareei, J., Rohani, A. and Mahmood, W.M.F.W., 2018. Simulation of a hydrogen/natural gas engine and modelling of engine operating parameters. International Journal of Hydrogen Energy, 43(25), pp.11639-11651.
62. Muniyappan, M., Prabakaran, S.T., Gopi, P., Shanmugam, M., Bhuvendran, A. and Shaisundaram, V.S., 2021. Hydrogen behavior in dual fuel mode diesel engine with nano diesel. Materials Today: Proceedings, 37, pp.2401-2405.
63. Castro, N., Toledo, M. and Amador, G., 2019. An experimental investigation of the performance and emissions of a hydrogen-diesel dual fuel compression ignition internal combustion engine. Applied Thermal Engineering, 156, pp.660-667.
64. Zareei, J., Rohani, A. and Alvarez, J.R.N., 2022. The effect of EGR and hydrogen addition to natural gas on performance and exhaust emissions in a diesel engine by AVL fire multi-domain simulation, GPR model, and multi-objective genetic

algorithm. international journal of hydrogen energy, 47(50), pp.21565-21581.

65. Chaichan, M.T., 2015. The effects of hydrogen addition to diesel fuel on the emitted particulate matters. International Journal of Scientific & Engineering Research, 6(6), pp.1081-1087.

66. Reddy, K.J., Rao, G.A.P., Reddy, R.M. and Aĝbulut, Ü., 2024. Artificial intelligence-based forecasting of dual-fuel mode CI engine behaviors powered with the hydrogen-diesel blends. International Journal of Hydrogen Energy, 87, pp.1074-1086.

67. Zhou, J.H., Cheung, C.S., Zhao, W.Z., Ning, Z. and Leung, C.W., 2015. Impact of intake hydrogen enrichment on morphology, structure and oxidation reactivity of diesel particulate. Applied Energy, 160, pp.442-455.

68. Frantzis, C., Zannis, T., Savva, P.G. and Yfantis, E.A., 2022. A review on experimental studies investigating the effect of hydrogen supplementation in CI diesel engines—The case of HYMAR. Energies, 15(15), p.5709.

69. Hernández, J.J., Cova-Bonillo, A., Wu, H., Barba, J. and Rodríguez-Fernández, J., 2022. Low temperature autoignition of diesel fuel under dual operation with hydrogen and hydrogen-carriers. Energy Conversion and Management, 258, p.115516.

70. Yan, F., Xu, L. and Wang, Y., 2018. Application of hydrogen enriched natural gas in spark ignition IC engines: from fundamental fuel properties to engine performances and emissions. Renewable and Sustainable Energy Reviews, 82, pp.1457-1488.

71. Wang, H., Ji, C., Shi, C., Wang, S., Yang, J. and Ge, Y., 2021. Investigation of the gas injection rate shape on combustion, knock and emissions behavior of a rotary engine with hydrogen direct-injection enrichment. International Journal of Hydrogen Energy, 46(27), pp.14790-14804.

72. Bhasker, J.P. and Porpatham, E., 2017. Effects of compression ratio and hydrogen addition on lean combustion characteristics and

emission formation in a Compressed Natural Gas fuelled spark ignition engine. Fuel, 208, pp.260-270.

73. Choi, G.H., Lee, J.C., Chung, Y.J., Caton, J. and Han, S.B., 2006. Effect of Hydrogen Enriched LPG Fuelled Engine with Converted from a Diesel Engine. Journal of Energy Engineering, 15(3), pp.139-145.